

## RESEARCH ARTICLE

# $\beta$ 1 integrin-mediated signaling regulates MT1-MMP phosphorylation to promote tumor cell invasion

Olivia R. Grafinger, Genya Gorshtein, Tyler Stirling, Megan I. Brasher and Marc G. Coppelino\*

## ABSTRACT

Malignant cancer cells can invade extracellular matrix (ECM) through the formation of F-actin-rich subcellular structures termed invadopodia. ECM degradation at invadopodia is mediated by matrix metalloproteinases (MMPs), and recent findings indicate that membrane-anchored membrane type 1-matrix metalloproteinase (MT1-MMP, also known as MMP14) has a primary role in this process. Maintenance of an invasive phenotype is dependent on internalization of MT1-MMP from the plasma membrane and its recycling to sites of ECM remodeling. Internalization of MT1-MMP is dependent on its phosphorylation, and here we examine the role of  $\beta$ 1 integrin-mediated signaling in this process. Activation of  $\beta$ 1 integrin using the antibody P4G11 induced phosphorylation and internalization of MT1-MMP and resulted in increased cellular invasiveness and invadopodium formation *in vitro*. We also observed phosphorylation of Src and epidermal growth factor receptor (EGFR) and an increase in their association in response to  $\beta$ 1 integrin activation, and determined that Src and EGFR promote phosphorylation of MT1-MMP on Thr<sup>567</sup>. These results suggest that MT1-MMP phosphorylation is regulated by a  $\beta$ 1 integrin-Src-EGFR signaling pathway that promotes recycling of MT1-MMP to sites of invadopodia formation during cancer cell invasion.

This article has an associated First Person interview with the first author of the paper.

**KEY WORDS:** Extracellular matrix, Integrin, MT1-MMP, Phosphorylation, Invadopodia

## INTRODUCTION

The process of metastasis is dependent on the ability of cells to invade the surrounding extracellular matrix (ECM) (Lu et al., 2012). In some malignant cell types, navigation through the ECM is facilitated by membrane protrusions known as invadopodia, which are F-actin-rich structures that facilitate cell invasion in both protease-independent and -dependent modes (Artym et al., 2009; Wisdom et al., 2018). During protease-independent invasion, invadopodia extend into the matrix and physically expand pores through contractile force (Wisdom et al., 2018). During protease-dependent invasion, the ECM is locally modified through the activity of adhesion receptors (integrins) and proteolytic enzymes (matrix metalloproteinases, MMPs). MMPs are able to digest a variety of ECM molecules, such as collagen, laminin and fibronectin, and the enzyme family is subdivided based on

substrate preference (Nagase et al., 2006). MMP enzymatic activity is dependent on the availability of zinc ions for the hydrolysis of peptide bonds within the ECM substrate (Nagase et al., 2006). MMPs are secreted as pro-enzymes and achieve full activation following cleavage of their pro-domain (Wang et al., 2004; Murphy and Courtneidge, 2011). Following activation, MMPs are either secreted from the cell or remain anchored to the cell surface where they carry out proteolytic functions (Murphy and Courtneidge, 2011). Of the membrane-anchored MMPs, membrane type 1-matrix metalloproteinase (MT1-MMP; also known as MMP14) is the most thoroughly characterized due to its importance in mediating ECM degradation in a variety of cancers (Moss et al., 2009b). Through its ECM remodeling activity MT1-MMP has been shown to activate a  $\beta$ 1 integrin signaling axis, and, accordingly, phosphorylation of FAK (PTK2) has been observed to be reduced in MT1-MMP knockout conditions (Tang et al., 2013). These data support the notion that a balance between adhesive and degradative activities is required for cellular invasion (Tang et al., 2013).

For a cell to maintain its invasive phenotype, MT1-MMP must be internalized and recycled to new sites of invadopodium formation (Nyalendo et al., 2007; Williams and Coppelino, 2011). Mutated forms of MT1-MMP lacking portions of the cytoplasmic domain lose the ability to be internalized, which consequently perturbs cell invasion (Lehti et al., 2000; Williams and Coppelino, 2011). Importantly, previous research has indicated that a reversible phosphorylation event on the cytoplasmic tail of MT1-MMP is sufficient to stimulate enzyme internalization from the cell surface and promote invasiveness (Nyalendo et al., 2007; Moss et al., 2009b; Williams and Coppelino, 2011). Thus, phosphorylation of MT1-MMP is potentially a key step in regulating metastasis; however, the signaling pathway regulating this phosphorylation remains unknown.

A possible mode of signaling that could play an important role in the regulation of MT1-MMP activity is that mediated through ECM adhesion. Adhesion to ECM components is mediated primarily by the integrin family of receptors, which physically link the matrix surrounding cells to the actin cytoskeleton and intracellular signal transduction pathways (Hynes, 2002; Guo and Giancotti, 2004; Destaing et al., 2010).  $\beta$ 1 integrin signaling has been found to play an important role in the establishment and maintenance of invadopodia in numerous cancer cell types (Nakahara et al., 1998; Murphy and Courtneidge, 2011; Beaty et al., 2013), and the activation of  $\beta$ 1 integrin has been shown to increase cellular invasiveness and matrix degradation at sites of invadopodium formation (Nakahara et al., 1998; Antelmi et al., 2013; Beaty et al., 2013). Previously, signaling from  $\beta$ 1 integrin receptors has been found to stimulate the formation of adhesive mechanosensory structures termed invadosomes, as well as to control ECM degradation at these sites (Destaing et al., 2011). Integrins have been shown to interact with several signaling molecules within cells (Wang et al., 1998; Moro et al., 2002; Beaty et al., 2013), and recently we characterized a complex containing  $\beta$ 1 integrin, Src

Department of Molecular and Cellular Biology, University of Guelph, Guelph, ON, N1G 2W1, Canada.

\*Author for correspondence (mcoppoli@uoguelph.ca)

DOI: 10.1242/jcs.239152

Handling Editor: Daniel Billadeau

Received 12 September 2019; Accepted 12 March 2020

kinase and epidermal growth factor receptor (EGFR), and described the function of this complex in invadopodium formation and tumor cell invasion (Williams and Coppolino, 2014).

In the present study, we examine the role of adhesion-based signaling in mediating MT1-MMP phosphorylation during invadopodia formation. We report that antibody-mediated activation of  $\beta 1$  integrin resulted in higher levels of MT1-MMP at the cell surface, consequently increasing invadopodia formation and cellular invasiveness. We found that Src kinase and EGFR were phosphorylated in response to  $\beta 1$  integrin stimulation and that the activation of these signaling molecules resulted in the phosphorylation of MT1-MMP on cytoplasmic Thr<sup>567</sup>. Phosphorylation of the enzyme resulted in increased internalization from the cell surface and subsequent recycling to sites of new invadopodia formation. These results provide a mechanistic framework for the regulation of MT1-MMP activity by  $\beta 1$  integrin during invadopodia formation in invasive tumor cells. The findings further suggest a role for crosstalk between  $\beta 1$  integrin and EGFR signaling in the regulation of invadopodia formation and function.

## RESULTS

### Activation of $\beta 1$ integrin promotes cell invasion and invadopodium formation

It has previously been shown that  $\beta 1$  integrin-mediated signaling plays an important role in many aspects of metastasis (Guo and Giancotti, 2004; Aoudjit and Vuori, 2012; Ganguly et al., 2013).

Here, we examined the role of integrin receptors during cell invasion and invadopodium formation. MDA-MB-231 cells were subjected to Matrigel invasion assays, using standard Boyden chambers, after treatment with antibodies to stimulate (P4G11) or inhibit (AIIB2)  $\beta 1$  integrin. The effects of antibody treatment on  $\beta 1$  integrin signaling were confirmed by analysis of FAK phosphorylation (Mitra and Schlaepfer, 2006). Treatment with the  $\beta 1$ -integrin-activating antibody increased FAK Y397 phosphorylation by  $89.6 \pm 16.7\%$  relative to the control (Fig. 1A,B). Additionally, the effect of antibody treatment on cellular spreading was analyzed and quantified to confirm that perturbation of the  $\beta 1$  integrin activation state had an effect on adhesive receptor function. In the presence of  $\beta 1$ -integrin-activating antibody, cells spread significantly more than the control, and in the presence of  $\beta 1$ -integrin-inactivating antibody cells demonstrated a significant reduction in spreading (Fig. 1C). Cell invasion was increased  $87.5 \pm 17.3\%$  after treatment with the  $\beta 1$ -integrin-activating antibody, whereas treatment with the  $\beta 1$ -integrin-inhibiting antibody decreased cellular invasion by  $45.5 \pm 6.2\%$ , compared with control (Fig. 1D). It is important to consider that the observed decrease in cell invasion associated with  $\beta 1$ -integrin-inactivating antibody treatment may partly result from cells adhering more slowly to the Matrigel substrate. Treatment with either activating or inhibitory  $\beta 1$  integrin antibodies had little effect on cell migration (data not shown). We hypothesized that the increased level of cellular invasion observed upon  $\beta 1$  integrin activation may be due to an increase in invadopodium formation.

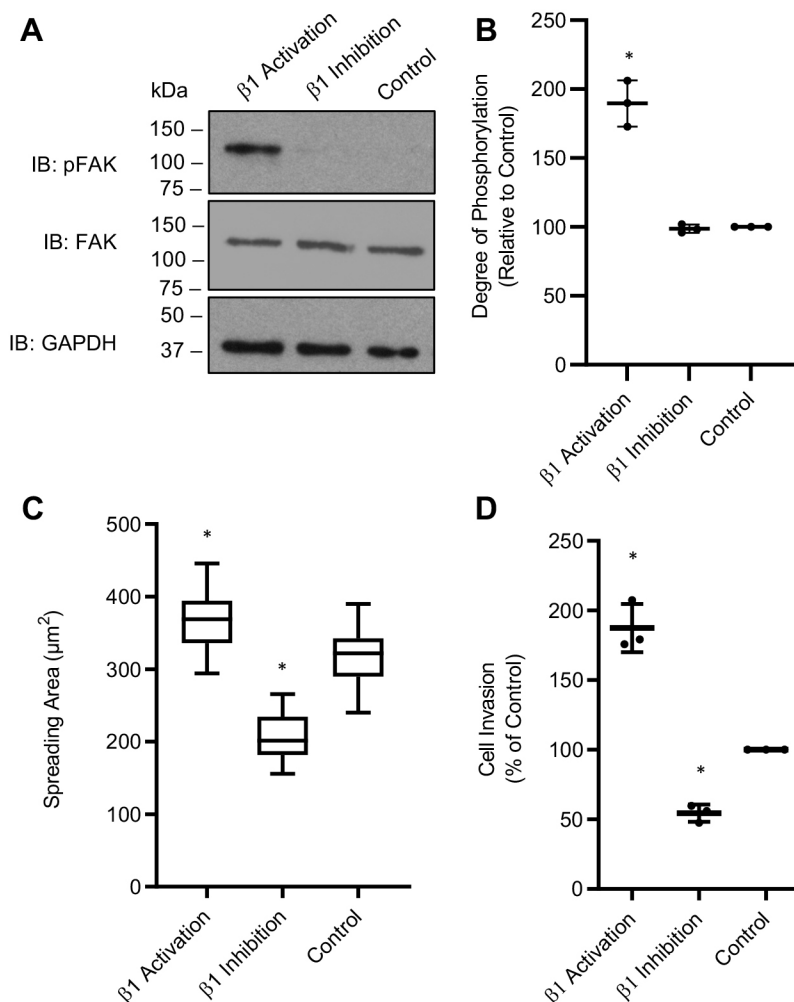


**Fig. 1. Activation of  $\beta 1$  integrin induces phosphorylation of FAK and stimulates cell spreading and invasion.**

(A) Analysis of FAK phosphorylation in whole cell lysates by western blot. Cells were plated onto gelatin and treated with AIIB2 and P4G11 for 2 h. Western blots show the amount of FAK-397 phosphorylation and GAPDH as loading control. Blots were then stripped and reprobed for FAK. (B) Densitometric analysis of pFAK from blots as shown in A, relative to the control. (C) Cells were plated onto gelatin-coated glass coverslips and treated with AIIB2 and P4G11 for 4 h. Cells were then fixed, permeabilized, and visualized by bright-field microscopy. Images obtained were used to quantify cell surface area for at least ten cells per treatment. (D) Quantification of cell invasion using Matrigel-coated transwell chambers. Serum-starved MDA-MB-231 cells were seeded onto wells, treated with AIIB2 or P4G11 antibody, and allowed to invade toward chemoattractant for 20 h. Percentages of cells are shown from three independent experiments in which ten fields of view were counted per treatment, and data are presented as percentage of control  $\pm$  s.d. Asterisks denote values significantly different from control (\* $P < 0.05$ ). All data represent three or more biological replicates with at least three technical replicates.

Using a fluorescent gelatin-based invadopodium formation assay (Williams et al., 2014), it was observed that treatment with  $\beta 1$ -integrin-activating antibody increased the number of cells forming invadopodia by  $97.4 \pm 16.0\%$  relative to the control (Fig. 2A,C). Staining of cells with an anti-active- $\beta 1$  integrin antibody revealed partial overlap of active  $\beta 1$  integrin with areas of gelatin degradation in cells treated with the  $\beta 1$ -integrin-activating antibody (Fig. S1). [Note that invadopodia are frequently disassembled/turned over, and therefore areas of gelatin degradation do not always align with F-actin punctae in captured images (Murphy and Courtneidge, 2011).] Analysis of subcellular distributions of cortactin and TKS5 (SH3PXD2A) by immunofluorescence microscopy revealed that activation of  $\beta 1$  integrin markedly increased the number of invadopodia precursors in cells (Fig. 2D, Fig. S2A) (Branch et al., 2012). A similar colocalization pattern was observed in cells stained for cortactin and vinculin (Fig. S2B). Incubation of cells on

fluorescent gelatin for a longer time period revealed that  $\beta 1$  integrin activation caused an increase in local ECM degradation compared with the control (Fig. 2B,E). Similar effects on invadopodium formation and ECM degradation were observed in HT-1080 fibrosarcoma cells treated with  $\beta 1$ -integrin-activating antibody (Fig. S3). Upon analyzing the abundance of the invadopodial proteins TKS5 and F-actin by western blot, we observed no significant difference in expression levels between treatments (data not shown).

### Activation of $\beta 1$ integrin increases expression of $\beta 1$ integrin and MT1-MMP at the cell surface, and secretion of MMPs

Previous studies have shown that  $\beta 1$  integrin signaling can influence trafficking of invadopodia components (Williams and Coppolino, 2014). We examined the distribution of  $\beta 1$  integrin and MT1-MMP, a key proteolytic enzyme localized to invadopodia during tumor cell invasion, in response to  $\beta 1$  integrin activation. A cell surface

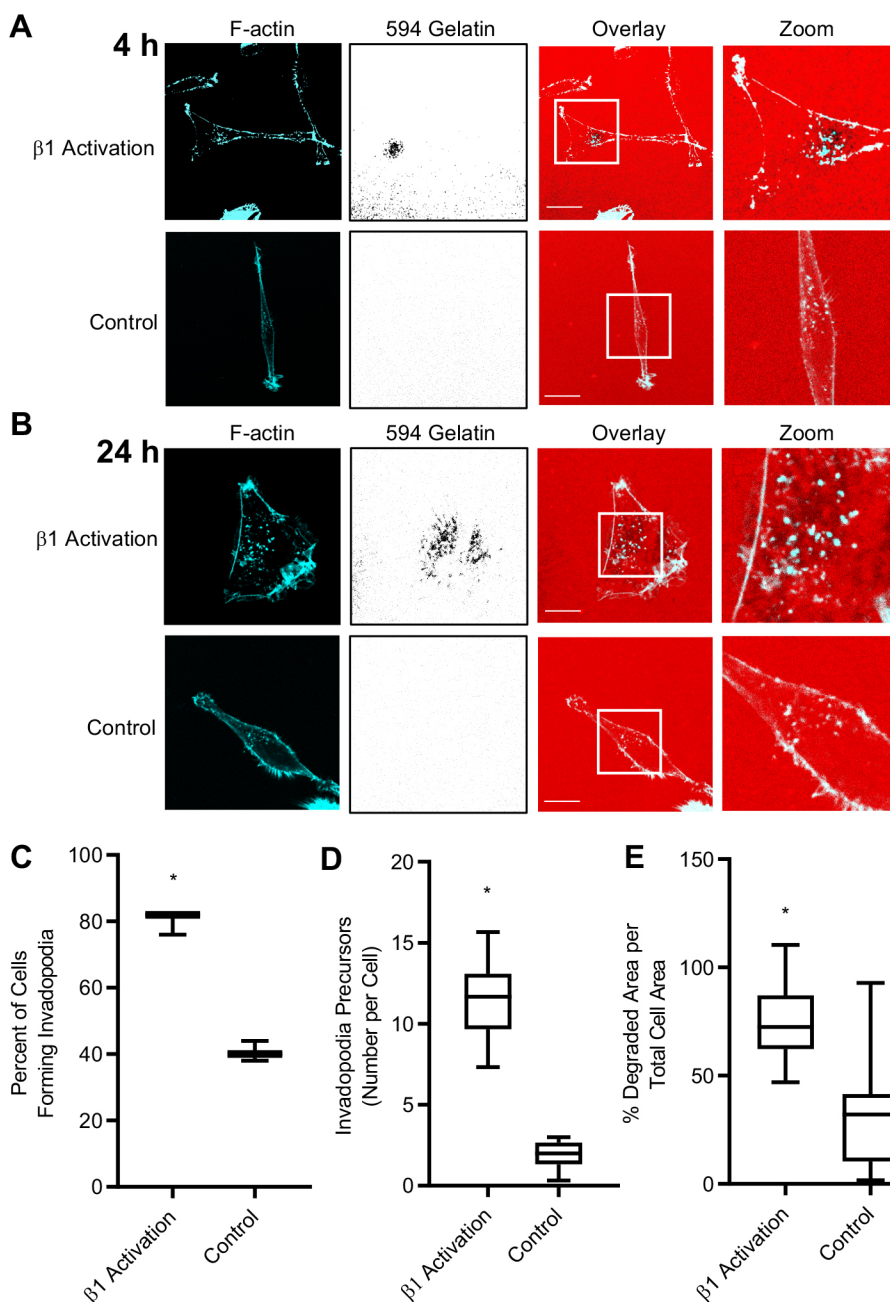


**Fig. 2. Invadopodium formation and gelatin degradation are increased when  $\beta 1$  integrin is activated.** (A,B) Cells were serum-starved, treated with P4G11, and plated on fluorescently labeled gelatin-coated coverslips for 4 h (A) or 24 h (B). Cells were then fixed, permeabilized, and stained for F-actin, and analyzed by confocal microscopy. Scale bars: 10  $\mu$ m. (C) Quantification of the invadopodium formation shown in A. (D) Quantification of invadopodia precursor formation using immunofluorescence microscopy. Serum-starved MDA-MB-231 cells were seeded onto gelatin-coated coverslips and incubated with AIB2 and P4G11 for 2 h. Colocalization of TKS5 and cortactin puncta were counted as invadopodia precursors, and the number of precursors were counted per cell. (E) Quantification of the gelatin degradation shown in B. In C, percentages of cells are shown from experiments in which 50 cells/sample were analyzed and normalized to the control condition. In E, areas of degradation were scored for ten cells per coverslip per treatment. All data represent three or more biological replicates with at least three technical replicates. Asterisks denote values significantly different from control (\* $P < 0.05$ ).



protein biotinylation assay was performed, and surface expression of  $\beta 1$  integrin and MT1-MMP were found to be increased by  $19.3 \pm 6.8\%$  and  $30.4 \pm 3.3\%$ , respectively, in  $\beta 1$ -integrin-activated cells compared with control (Fig. 3A,B). Treatment with the  $\beta 1$ -integrin-inhibiting antibody did not alter the cell surface level of MT1-MMP (data not shown). Similar changes in surface MT1-MMP expression in response to  $\beta 1$  integrin activation were also observed in HT-1080 cells (data not shown). In agreement with our biotinylation data, examination of  $\beta 1$ -integrin-activated cells by epifluorescence microscopy revealed visibly increased cell surface levels of MT1-MMP and  $\beta 1$  integrin colocalized at discrete punctae (Fig. 3C). Additionally, we observed increased levels of secreted MMP2, MMP9 and proMMP9 in these cells using gelatin zymography (Fig. 3D). Thus, the increased level of invadopodium formation observed in  $\beta 1$ -integrin-activated cells correlates with higher levels of cell surface MT1-MMP and of secreted MMPs required for ECM degradation.

### MT1-MMP is phosphorylated and internalized in a $\beta 1$ integrin-dependent manner

During the process of cell invasion, invadopodia are disassembled and reformed at the leading edge of the cell, and in cells plated on a 2D substrate this is typically observed at the ventral surface, often under the nucleus (Murphy and Courtneidge, 2011). The dynamic nature of invadopodium formation requires that cells recycle MT1-MMP, and it has been determined that the phosphorylation of MT1-MMP is crucial for regulating its intracellular recycling (Lehti et al., 2000; Williams and Coppolino, 2011). We hypothesized that  $\beta 1$  integrin activation may influence MT1-MMP phosphorylation and its internalization from the cell surface. Western blots with phospho-Ser/Thr-specific antibodies revealed that activation of  $\beta 1$  integrin resulted in increased phosphorylation of MT1-MMP after 2 h (Fig. 4A), as well as at 40 min and 4 h time points (data not shown). MT1-MMP immunoprecipitates were also probed for phospho-Tyr and a

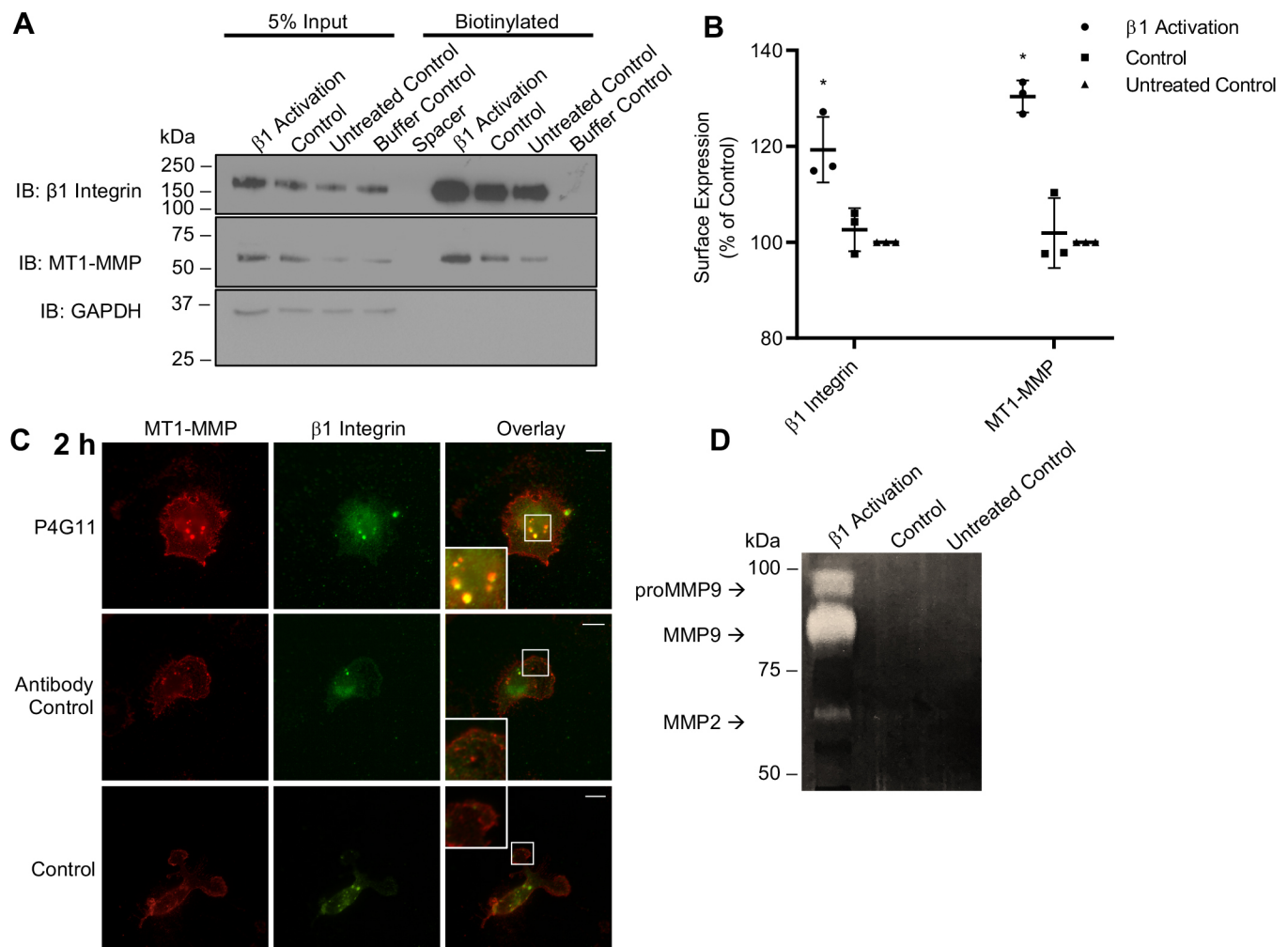


**Fig. 3.  $\beta 1$  integrin activation increases cell surface levels of integrin and MT1-MMP.** (A) Streptavidin pull-downs of biotinylated proteins from surface-labeled MDA-MB-231 cells plated on gelatin, with or without treatment with P4G11 for 2 h. Western blots show amounts of  $\beta 1$  integrin and MT1-MMP captured, and GAPDH as loading control for inputs. Control cells were treated with a non-specific supernatant antibody, untreated control cells were not exposed to antibody, and buffer control cells were exposed to buffer without biotin. (B) Densitometric analysis of the amount of cell surface  $\beta 1$  integrin and MT1-MMP as shown in A, relative to the control condition. Data are presented as percentage of control  $\pm$  s.d. Asterisks denote values significantly different from the control condition (\* $P < 0.05$ ). (C) Serum-starved cells were plated onto gelatin-coated coverslips for 2 h with or without P4G11 treatment, then were fixed and stained using antibodies to MT1-MMP and  $\beta 1$  integrin. Cells were visualized by epifluorescence microscopy, and representative images are shown. Scale bars: 10  $\mu$ m. (D) Gelatin zymographs showing MMP2, MMP9 and proMMP9 activity in serum-starved MDA-MB-231 cells treated with P4G11 and plated onto gelatin for 16 h. All data represent three or more biological replicates with at least three technical replicates.



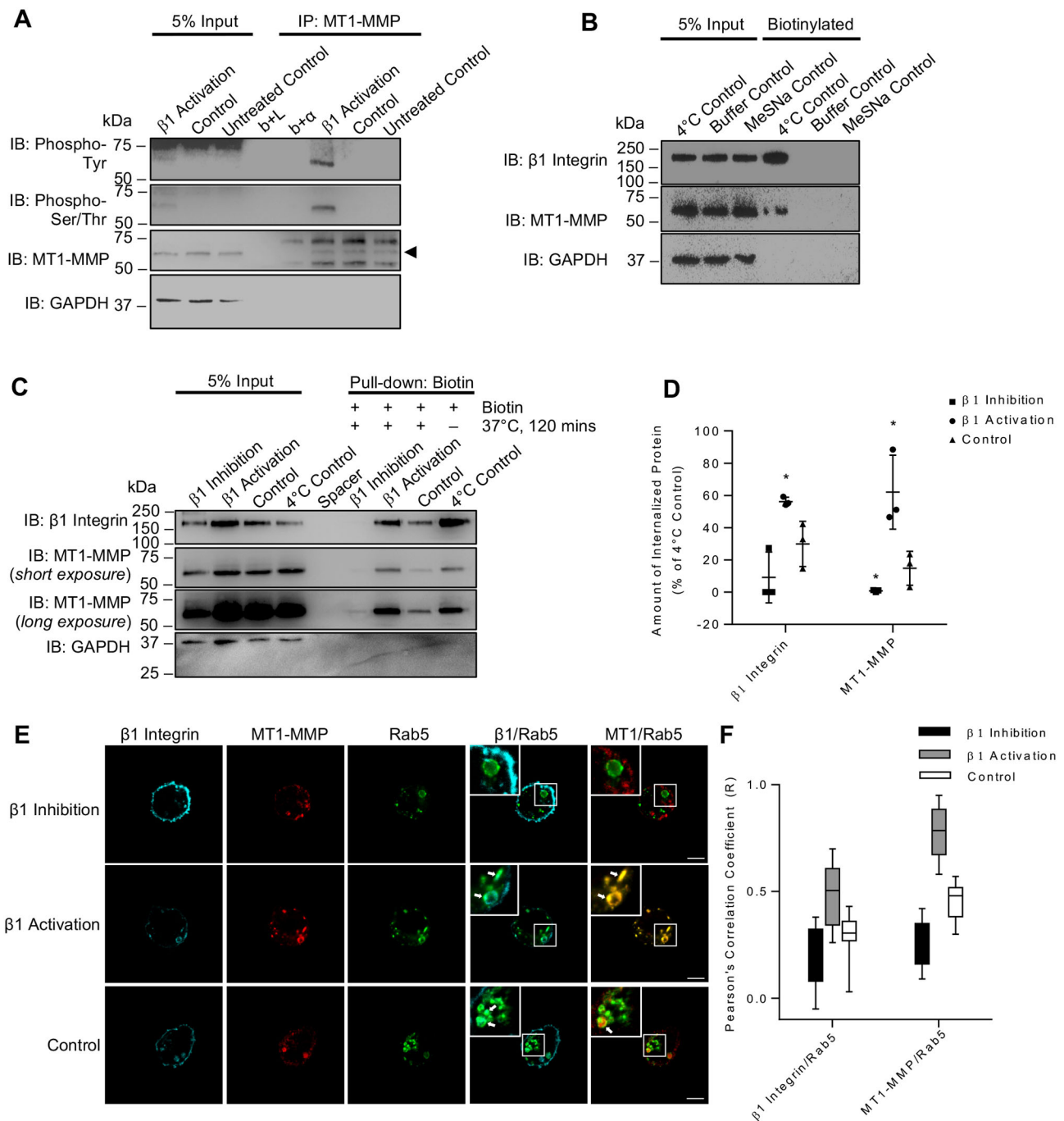


**Fig. 4. Activation of  $\beta 1$  integrin induces phosphorylation and intracellular trafficking of MT1-MMP.** (A) Immunoprecipitation of MT1-MMP from MDA-MB-231 cells. Cells were plated onto gelatin-coated cell culture plates for 2 h, with or without treatment with P4G11, and immunoprecipitates of MT1-MMP were analyzed by western blot for phospho-Ser/Thr and phospho-Tyr. Blots were stripped and re-probed for MT1-MMP. Control cells were treated with a non-specific supernatant antibody, untreated control cells were not exposed to antibody. b+L, beads plus lysate; b+ $\alpha$ , beads plus antibody. Arrowhead indicates the active form of MT1-MMP recognized by the anti-MT1-MMP antibody. (B,C) MT1-MMP is internalized when  $\beta 1$  integrin signaling is activated. Serum-starved MDA-MB-231 cells were plated on gelatin for 2 h and surface labeled with biotin. Biotinylated cells were then incubated at 37°C to allow internalization of labeled proteins, with or without antibody treatment. Following incubation, cells were treated with MeSNa to remove any biotin-labeled proteins remaining at the cell surface, and internalized biotinylated proteins were pulled out of the lysate using streptavidin-coated beads. Western blots show amounts of internalized  $\beta 1$  integrin and MT1-MMP captured, and GAPDH as loading control for inputs. 4°C control cells were treated with both biotin and borate buffer, buffer control cells were exposed to buffer only, MeSNa control cells were treated with MESNA immediately following surface labeling, control cells were treated with a non-specific supernatant antibody. (D) Quantification of internalized  $\beta 1$  integrin and MT1-MMP as shown in C, relative to the 4°C control condition. Data are presented as percentage of 4°C control  $\pm$  s.d. Asterisks denote values significantly different from the 4°C control condition ( $*P < 0.05$ ). (E) MDA-MB-231 cells expressing Rab5-GFP were serum-starved overnight and plated onto gelatin for 2 h. Cell surface MT1-MMP and  $\beta 1$  integrin were labeled using antibodies at 4°C, followed by incubation at 37°C for 40 min to allow internalization. Cells were fixed, permeabilized and stained, and protein localization following internalization was analyzed by confocal microscopy. Insets show magnification of the boxed areas. White arrows indicate overlay of proteins. (F) Colocalization of MT1-MMP or  $\beta 1$  integrin with Rab5-GFP was quantified as a Pearson's correlation coefficient and represented graphically ( $n = 10$  cells per treatment). Asterisks denote values significantly different from the control condition ( $*P < 0.05$ ). Data represent three or more biological replicates with at least three technical replicates. Scale bars: 10  $\mu$ m.

similar effect on MT1-MMP phosphorylation was observed (Fig. 4A). Similar changes in MT1-MMP phosphorylation in response to activation of  $\beta 1$  integrin were observed in cells plated on fibronectin and collagen substrates, as well as in HT-1080 cells plated on gelatin (Fig. S4). [Note that three forms of MT1-MMP exist (pro-form, active form and cleaved form), which are recognized by the antibody and enriched in immunoprecipitates, appearing as three distinct bands when blots are stripped and re-probed for MT1-MMP (Bernardo and Fridman, 2003).] Additionally, a reverse immunoprecipitation of phospho-Ser/Thr from cell lysates revealed an increase in eluted MT1-MMP following  $\beta 1$  integrin activation (Fig. S5).

To assess internalization of MT1-MMP, a modified cell surface biotinylation assay was performed, as described previously (Remacle et al., 2003), utilizing the membrane-impermeable reducing agent sodium 2-mercaptoethanesulfonate (MeSNa) (Fig. 4B,C). In this protocol, detection of internalized proteins is achieved through the external application of biotin to label proteins on the cell surface; incubation of cells, followed by cleavage of surface biotin label with MeSNa allows detection of only biotin-labeled proteins that had been internalized. Treatment with  $\beta 1$ -integrin-activating antibody for 2 h resulted in the internalization of  $56.2 \pm 2.6\%$  of  $\beta 1$  integrin and  $62.1 \pm 22.9\%$  of MT1-MMP from the cell surface, significantly more than both the control and  $\beta 1$ -integrin-inhibited cells (Fig. 4D). Examination of MT1-MMP and  $\beta 1$  integrin intracellular trafficking by confocal microscopy yielded results consistent with these biochemical data, revealing a visible increase in MT1-MMP and  $\beta 1$  integrin association with the early endosome marker Rab5 (Fig. 4E). Quantification of protein colocalization was performed using data taken from images of multiple cells from multiple replicates, and it was observed that in  $\beta 1$ -integrin-activated cells MT1-MMP and  $\beta 1$  integrin colocalized with Rab5 at 40 min (Pearson's correlations of  $0.78 \pm 0.13$  and  $0.48 \pm 0.15$ , respectively) (Fig. 4F). It was also observed that MT1-MMP and  $\beta 1$  integrin colocalized with Rab7, a late endosome marker, at 2 h with Pearson's correlations of  $0.52 \pm 0.17$  and  $0.41 \pm 0.11$ , respectively (data not shown). These results suggest that activation of  $\beta 1$  integrin promotes the phosphorylation of MT1-MMP and its internalization from the cell surface, where it is trafficked through early endosomes marked by Rab5 and late endosomes marked by Rab7.

#### Association of Src, EGFR and $\beta 1$ integrin is enhanced downstream of $\beta 1$ integrin activation

It is well documented that  $\beta 1$  integrin associates with Src kinase and EGFR to facilitate their activation during tumor cell invasion (Moro et al., 2002; Williams and Coppolino, 2014). We hypothesized that antibody-mediated activation of  $\beta 1$  integrin induces association of these proteins, and analyzed this by co-immunoprecipitation and immunofluorescence microscopy. Probing of Src immunoprecipitates by western blot revealed increased amounts of both  $\beta 1$  integrin and EGFR as a result of treatment with  $\beta 1$ -integrin-activating antibody (Fig. 5A). Src association with  $\beta 1$  integrin was quantified and found to have increased by  $51.6 \pm 10.6\%$ , and association with EGFR by  $36.5 \pm 12.7\%$ , as a result of antibody treatment (Fig. 5B). Immunoprecipitation of  $\beta 1$  integrin resulted in similar observations, with co-immunoprecipitation of EGFR and Src being increased over the control condition by  $36.2 \pm 8.5\%$  and  $39.3 \pm 13.7\%$ , respectively, as a result of integrin activation by P4G11 treatment (Fig. S6). Consistent with the co-immunoprecipitation of these proteins, immunofluorescent microscopic examination of Src,  $\beta 1$  integrin and EGFR with the invadopodia marker cortactin revealed

that these signaling molecules associate at distinct invadopodial punctae when  $\beta 1$  integrin signaling is activated (Fig. 5C).

#### EGFR is phosphorylated downstream of $\beta 1$ integrin in a Src kinase-dependent manner

Previous findings have shown that integrin-mediated adhesion can activate growth factor receptors, independently of growth factor binding (Moro et al., 1998, 2002; Kuwada and Li, 2000; Yu et al., 2000). Here, we tested the effect of  $\beta 1$  integrin activation on the phosphorylation of Src kinase and EGFR in MDA-MB-231 cells (Fig. 6A,B). Cells treated with the  $\beta 1$ -integrin-activating antibody had a  $25.6 \pm 6.2\%$  increase in Src phosphorylation, relative to control (Fig. 6C). These cells also displayed a  $35.5 \pm 2.6\%$  increase in tyrosine phosphorylation of EGFR (Fig. 6D).

To test if EGFR phosphorylation is downstream of Src, cells were treated with an inhibitor of Src family kinases, PP2, in combination with the  $\beta 1$ -integrin-activating antibody (Fig. 6E). Treatment with PP2 significantly decreased tyrosine phosphorylation of EGFR in response to  $\beta 1$  integrin activation by  $24.8 \pm 2.2\%$  (Fig. 6G). To verify the involvement of Src in EGFR phosphorylation, MDA-MB-231 cells were transfected with Src phospho-mutant constructs, exposed to  $\beta 1$ -integrin-activating antibody, and phosphorylation of EGFR was then analyzed (Fig. 6F). Expression of a constitutively active Src mutant (Y529F) increased tyrosine phosphorylation of EGFR by  $30.9 \pm 16.9\%$  over control (Fig. 6H). Expression of dominant-negative Src (K296R/Y528F) had the opposite effect; EGFR phosphorylation was decreased by  $23.7 \pm 15.0\%$  compared with control (Fig. 6H). These results suggest that activation of  $\beta 1$  integrin stimulates Src kinase, which can subsequently lead to phosphorylation of EGFR.

#### $\beta 1$ integrin-stimulated phosphorylation of MT1-MMP is dependent on Src, EGFR and FAK activity

The observations that  $\beta 1$  integrin activation led to phosphorylation of MT1-MMP, and to the activation of Src kinase and EGFR, suggest that Src and EGFR may be involved in the signaling pathway leading to MT1-MMP phosphorylation. To test this, MDA-MB-231 cells were treated with  $\beta 1$ -integrin-activating antibody, in combination with either the Src inhibitor PP2 or the EGFR inhibitor AG1478, and phosphorylation of MT1-MMP was analyzed by immunoprecipitation-western blot. Phosphorylation of MT1-MMP in response to  $\beta 1$  integrin activation was strongly reduced when Src was inhibited (Fig. 7A,B). MT1-MMP phosphorylation induced by  $\beta 1$ -integrin-activating antibody was similarly reduced in cells treated with AG1478 (Fig. 7C,D). Treatment of cells with EGF alone did result in phosphorylation of MT1-MMP, further supporting a requirement for EGFR signaling in the phosphorylation of the enzyme (Fig. 7E). The requirement for Src kinase function was also tested by transfecting cells with a pool of siRNAs targeting Src, or a nonspecific control siRNA. Knockdown of Src was observed after 48 h; endogenous levels of the protein were reduced by  $62.7 \pm 10.7\%$  (Fig. S7A,B). Knockdown of Src kinase had a substantial effect on EGFR activation following integrin activation, decreasing tyrosine phosphorylation of the receptor by  $65.6 \pm 2.7\%$  relative to the control siRNA condition (Fig. S8C). Analysis by immunoprecipitation revealed that knockdown of Src resulted in decreased phosphorylation of MT1-MMP by  $77.3 \pm 6.0\%$  compared with control (Fig. S7D,E). FAK knockdown by RNAi resulted in a  $74.4 \pm 13.8\%$  decrease in endogenous protein levels, and this led to a similar decrease in MT1-MMP phosphorylation (Fig. S7F). These findings suggest that Src, EGFR and FAK act downstream of  $\beta 1$  integrin and are necessary for  $\beta 1$  integrin-stimulated phosphorylation of MT1-MMP.

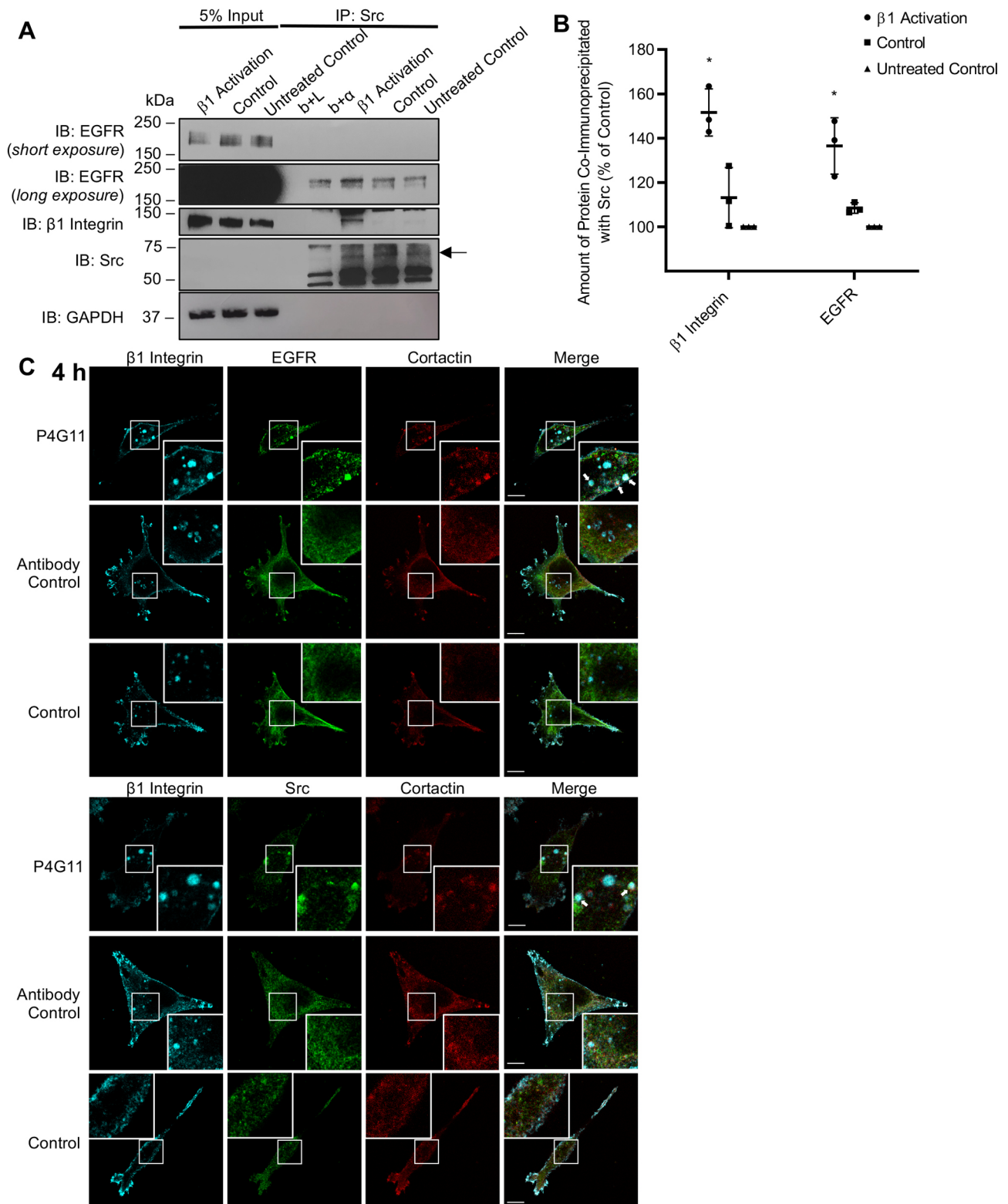


**Fig. 5.  $\beta 1$  integrin activation increases the colocalization and association of invadopodial proteins.** (A,B) Serum-starved MDA-MB-231 cells were plated onto gelatin for 2 h with or without treatment with P4G11. (A) Immunoprecipitates of Src kinase were analyzed for association with  $\beta 1$  integrin and EGFR by western blot. Arrow indicates Src recognized by the anti-Src antibody. Control cells were treated with a non-specific supernatant antibody, untreated control cells were not exposed to antibody. b+L, beads plus lysate; b+ $\alpha$ , beads plus antibody. (B) Quantification of the amount of co-immunoprecipitated proteins presented in A. Data are expressed as percentage of control  $\pm$  s.d. Asterisks denote values significantly different from the control condition ( $*P < 0.05$ ). Data represent three or more biological replicates with at least three technical replicates. (C) Serum-starved cells were plated onto gelatin-coated coverslips for 4 h with or without P4G11 treatment then fixed, permeabilized and stained for either  $\beta 1$  integrin (antibody P4C10) and EGFR (top), or  $\beta 1$  integrin and Src (bottom). Cells were analyzed by confocal microscopy and representative sections from the ventral region of cells are shown. Insets show magnification of the boxed areas. White arrows indicate overlay of all three stained proteins. Scale bars: 10  $\mu$ m.



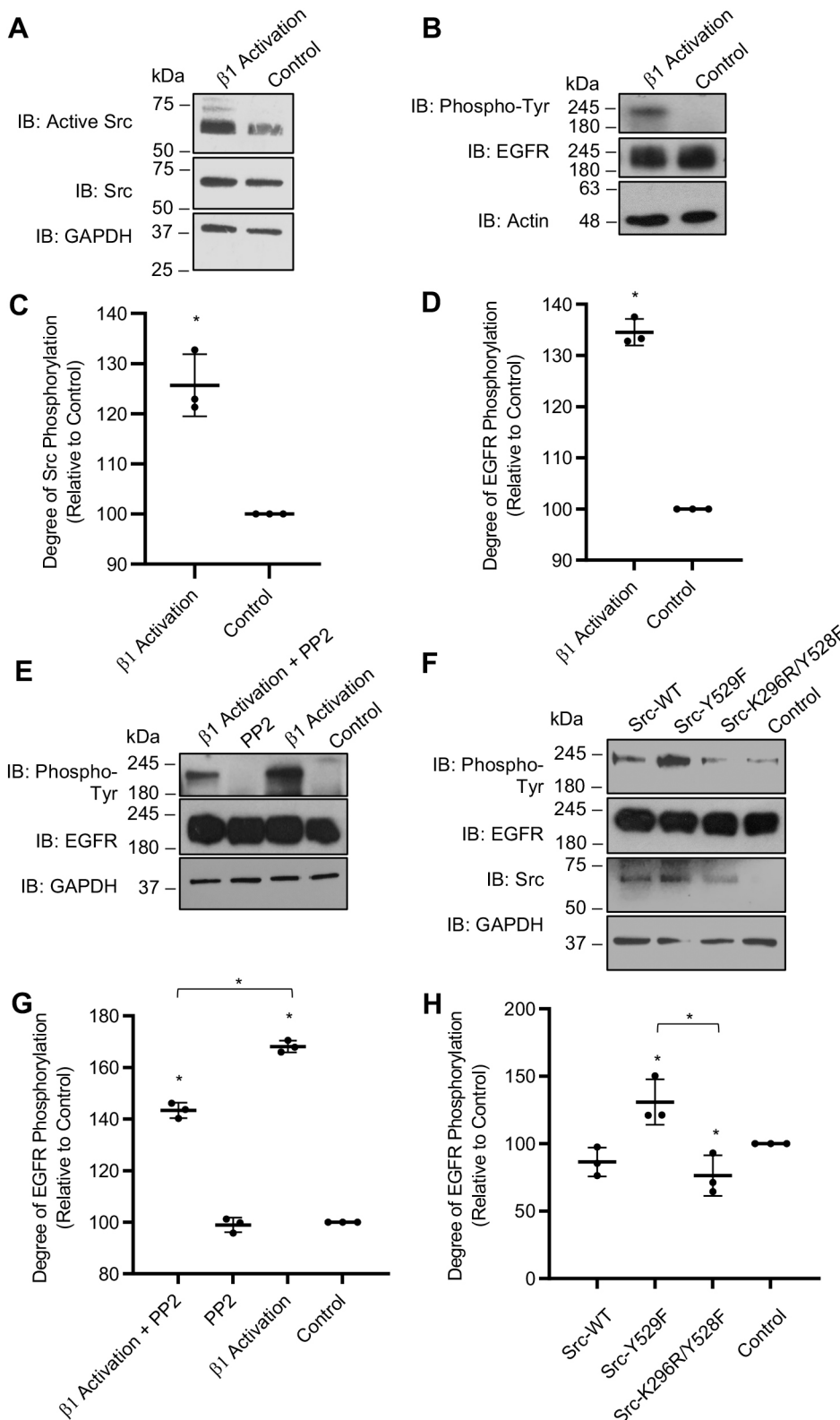


**Fig. 6.  $\beta$ 1 integrin stimulation induces the phosphorylation of Src kinase and subsequent activation of EGFR.**

(A–D) Serum-starved cells were plated onto gelatin with or without treatment of P4G11 for 2 h and then lysed. Whole cell lysates were analyzed by western blot for phosphorylation of Src (A) and EGFR (B), and blots were then stripped and re-probed for Src and EGFR. (C,D) Densitometric analysis of Src kinase and EGFR phosphorylation as shown in A and B. (E–H) Analysis of EGFR tyrosine phosphorylation in whole cell lysates by western blot. (E) Cells were plated onto gelatin and treated with P4G11, PP2, or a combination of both, for 2 h. Blots were probed for phospho-Tyr, and then stripped and re-probed for EGFR. Control cells were treated with a non-specific supernatant antibody. (F) Cells were transiently transfected with Src-WT, Src-Y529F or Src-K296R/Y528F, plated on gelatin, treated with P4G11, and analyzed as in E. Blots were probed for phospho-Tyr and Src kinase, and then stripped and re-probed for EGFR. Control cells were untransfected and treated with P4G11. (G,H) Quantification of phospho-Tyr as shown in E and F. GAPDH served as loading control in A,E,F; F-actin is loading control in B. Data are presented as percentage of control  $\pm$  s.d. Asterisks denote values significantly different from the control condition (\* $P$ <0.05). All data represent three or more biological replicates with at least three technical replicates.

### MT1-MMP is phosphorylated on Thr<sup>567</sup> downstream of $\beta$ 1 integrin activation

Previously, it has been shown that phosphorylation of MT1-MMP on Thr<sup>567</sup> of its cytoplasmic domain is important for enzyme internalization and, consequently, cell invasion (Uekita et al., 2001; Williams and Coppolino, 2011). We hypothesized that if  $\beta$ 1 integrin activation induces phosphorylation of MT1-MMP on

Thr<sup>567</sup>, then expression of a mutant construct that is non-phosphorylatable at this residue may impair the ability of cells to form invadopodia. Using the invadopodia formation assay as above, we observed that expression of T567A-MT1-MMP-GFP decreased the number of cells forming invadopodia by  $63.1 \pm 6.8\%$  compared with the control (Fig. 8A,B). Incubation of cells on the fluorescent gelatin substrate for a longer time period revealed a

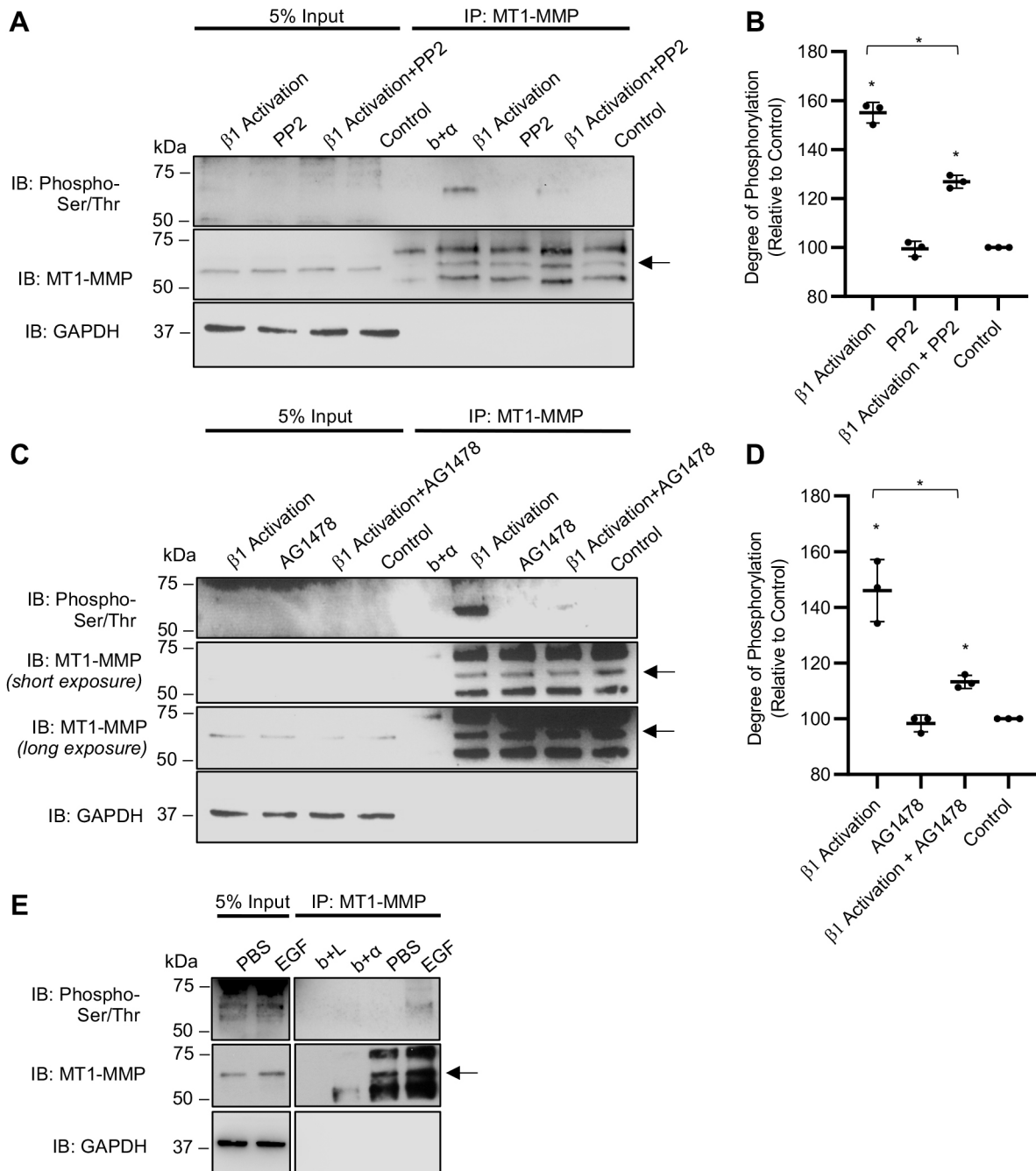


**Fig. 7. Inhibition of Src or EGFR decreases MT1-MMP phosphorylation when  $\beta 1$  integrin is activated.** (A,C) Immunoprecipitation of MT1-MMP from MDA-MB-231 cells treated with (A) P4G11, PP2, or a combination of both, or (C) P4G11, AG1478, or a combination of both. Western blots were probed for phospho-Ser/Thr, and then stripped and re-probed for MT1-MMP. Control cells were treated with a non-specific supernatant antibody. b+ $\alpha$ , beads plus antibody. (B,D) Quantification of phospho-Ser/Thr as shown in A and C. (E) Serum-starved MDA-MB-231 cells were plated onto gelatin and treated with either EGF or PBS (vehicle) for 2 h prior to being lysed. Immunoprecipitates of MT1-MMP were analyzed for phospho-Ser/Thr, then stripped and re-probed for MT1-MMP by western blot. Arrows indicate the active form of MT1-MMP recognized by the anti-MT1-MMP antibody. In A,C,E, GAPDH served as loading controls. All data are presented as percentage of control  $\pm$  s.d. Asterisks denote values significantly different from the control condition ( $*P < 0.05$ ). All data represent three or more biological replicates with at least three technical replicates.

substantial decrease in local ECM degradation in cells transfected with T567A-MT1-MMP-GFP (Fig. 8C). By contrast, minimally observable changes in invadopodium formation and gelatin degradation were seen in cells expressing an MT1-MMP construct with Tyr<sup>573</sup> mutated to alanine (Y573A-MT1-MMP-GFP) (Fig. 8A,C). In cells expressing both WT-MT1-MMP-GFP and Y573A-MT1-MMP-GFP, strongly overlapping distributions

of the mutant constructs with the invadopodia markers cortactin and  $\beta 1$  integrin were observed. Interestingly, in cells expressing T567A-MT1-MMP-GFP colocalization of the mutant construct with cortactin and  $\beta 1$  integrin was not observed (Fig. S8). Western blot analysis of GFP immunoprecipitates showed a  $56.5 \pm 3.9\%$  decrease in MT1-MMP Ser/Thr phosphorylation in cells expressing T567A-MT1-MMP-GFP, despite treatment of cells

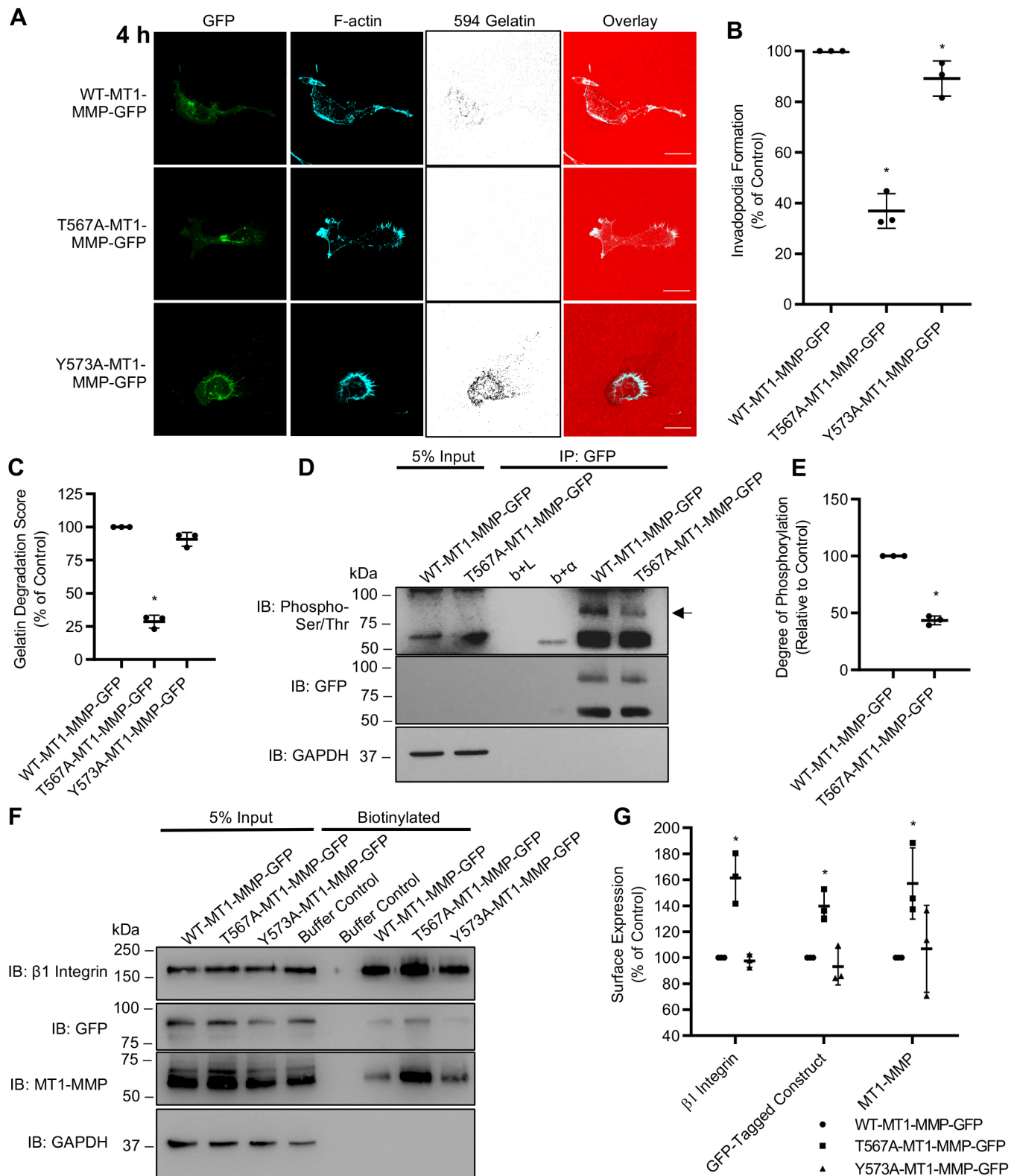


Fig. 8. See next page for legend.

with  $\beta$ 1-integrin-activating antibody (Fig. 8D,E). Importantly, expression of T567A-MT1-MMP-GFP led to increased cell surface expression of the mutant MT1-MMP, as well as  $\beta$ 1 integrin and endogenous MT1-MMP, by  $39.7 \pm 11.8\%$ ,  $61.4 \pm 19.4\%$  and  $57.1 \pm 27.5\%$ , respectively (Fig. 8F,G). These results are

consistent with previous findings indicating that phosphorylation of MT1-MMP at Thr<sup>567</sup> regulates its intracellular trafficking, which is coupled to integrin trafficking (Williams and Coppolino, 2011). Together, our observations suggest that activation of  $\beta$ 1 integrin induces phosphorylation of MT1-MMP on Thr<sup>567</sup>, and



**Fig. 8. MT1-MMP is phosphorylated on Thr<sup>567</sup> downstream of  $\beta$ 1 integrin activation.** (A) Cells transfected with WT-MT1-MMP-GFP, T567A-MT1-MMP-GFP or Y573A-MT1-MMP-GFP were serum-starved, treated with P4G11, and plated on fluorescently labeled gelatin-coated coverslips for 4 h. Cells were then fixed, permeabilized, stained for F-actin, and analyzed by confocal microscopy. Scale bars: 10  $\mu$ m. (B) Quantification of the invadopodium formation shown in A. Transfected cells forming F-actin punctae overlaying dark spots of gelatin degradation were counted. (C) Quantification of 16 h gelatin degradation. Areas of gelatin degradation were analyzed microscopically and scored. In B and C, percentages of cells are shown from experiments in which 50 cells/sample were analyzed and normalized to the control condition. (D) Immunoprecipitation of GFP-tagged constructs from MDA-MB-231 cells. Transfected cells were plated onto gelatin-coated cell culture plates for 2 h, with treatment of P4G11, and immunoprecipitates carried out with an antibody to GFP were analyzed by western blot for phospho-Ser/Thr, followed by stripping and re-probing for GFP. Arrows indicate GFP-tagged constructs recognized by the anti-phospho-Ser/Thr and anti-GFP antibodies. b+L, beads plus lysate; b+ $\alpha$ , beads plus antibody. (E) Densitometric analysis of MT1-MMP phosphorylation as shown in D. (F) Transfected cells were plated onto gelatin-coated plates for 2 h, treated with P4G11, and streptavidin pull-downs of biotinylated proteins were analyzed by western blot to show the relative amounts of cell surface proteins. Buffer control cells were exposed to buffer without biotin. (G) Densitometric analysis of the amount of cell surface  $\beta$ 1 integrin, MT1-MMP construct, and endogenous MT1-MMP as shown in F, relative to the WT-MT1-MMP-GFP condition. In D and F, GAPDH was used as loading control. All data are presented as percent of control  $\pm$ s.d. All data represent three or more biological replicates with at least three technical replicates. Asterisks denote values significantly different from control (\* $P$ <0.05).

that this phosphorylation event is important for the expression of an invasive phenotype.

## DISCUSSION

Studies of tumor cell invasion have revealed the important role that MT1-MMP plays in proteolytic degradation of the ECM, and metastatic progression (Moss et al., 2009b). It has been established that endocytosis and recycling of the enzyme to sites of invadopodium formation are necessary for a cell to maintain its invasiveness (Moss et al., 2009b; Williams and Coppelino, 2011). Truncation of the enzyme's cytoplasmic domain has been shown to lead to its enrichment on the plasma membrane, indicating a role for this domain in the regulation of the enzyme's internalization and trafficking (Lehti et al., 2000; Uekita et al., 2001). The 20 amino acid cytoplasmic domain of MT1-MMP contains three potential phosphorylation sites (Thr<sup>567</sup>, Tyr<sup>573</sup> and Ser<sup>577</sup>), and further study determined that phosphorylation of the enzyme is necessary for its endocytosis and recycling (Nyalendo et al., 2007; Moss et al., 2009a,b; Williams and Coppelino, 2011). Results reported here suggest that  $\beta$ 1 integrin-mediated signaling plays a role in the control of MT1-MMP cell surface expression, and accordingly the invasive capacity of tumor cells. We propose a model wherein this  $\beta$ 1 integrin-mediated signaling regulates the phosphorylation of MT1-MMP in a manner that is dependent on EGFR, Src and FAK.

Using modified Boyden chamber and gelatin degradation assays, we observed that activation of  $\beta$ 1 integrin with the antibody P4G11 increases cellular invasion along with invadopodium formation. MT1-MMP is reported to be enriched in the invadopodia of numerous invasive cancer cell types (Weaver, 2006; Poincloux et al., 2009; Frittoli et al., 2011; Beaty and Condeelis 2014; Williams and Coppelino, 2014), and we therefore hypothesized that the observed differences in cellular invasiveness may result, in part, from increased surface expression of MT1-MMP in  $\beta$ 1-integrin-activated cells. We found that activation of  $\beta$ 1 integrin led to increased cell surface expression of MT1-MMP, as well as enhanced secretion of the soluble enzymes MMP2, MMP9 and

proMMP9. These effects are consistent with the observed increases in gelatin degradation and cell invasion that resulted from  $\beta$ 1 integrin activation. MT1-MMP is known to be a potent activator of MMP2 and MMP9 through cleavage of their pro-domains, and this action contributes to increased proteolytic activity at the cell surface during cell invasion (Deryugina et al., 2001; Toth et al., 2003).

Our observations suggest the activity of  $\beta$ 1 integrin supports the development of invadopodia by stimulating the recycling MT1-MMP, a key component of invadopodia. Previous work indicates that phosphorylation of MT1-MMP promotes its internalization and subsequent delivery to sites of invadopodium formation (Remacle et al., 2003; Nyalendo et al., 2007; Williams and Coppelino, 2011). Here, we find that activation of  $\beta$ 1 integrin by P4G11 antibody treatment stimulates phosphorylation of MT1-MMP, in both MDA-MB-231 cells and HT-1080 cells. Future studies utilizing non-functional  $\beta$ 1 integrin mutant constructs as well as  $\beta$ 1 integrin knockout cell lines are planned to investigate further the specificity of  $\beta$ 1 integrin signaling on the internalization and phosphorylation of MT1-MMP. We do report that increased MT1-MMP phosphorylation coincided with increased internalization of the enzyme, consistent with previous findings (Nyalendo et al., 2007; Moss et al., 2009b; Williams and Coppelino, 2011), and trafficking of both MT1-MMP and  $\beta$ 1 integrin through early and late endosomes. As increased levels of cell surface MT1-MMP were detected under these conditions, it is thus possible that intracellular pools of MT1-MMP are being diverted from degradative pathways and trafficked to the cell surface. It is also possible that observed increases in  $\beta$ 1 integrin and MT1-MMP at the cell surface in  $\beta$ 1-integrin-activated cells may result from an association of the two proteins at the cell surface, as it has previously been shown that MT1-MMP has the ability to interact with integrin subunits (Deryugina et al., 2001; Gálvez et al., 2002).

The phosphorylation of MT1-MMP was detected using anti-phosphotyrosine and anti-phosphoserine/threonine antibodies; however, the use of non-phosphorylatable mutant constructs suggests that the phenotype caused by activation of  $\beta$ 1 integrin primarily results from phosphorylation of the enzyme on residue Thr<sup>567</sup>. Accumulation of T567A-MT1-MMP-GFP at the cell surface is consistent with previous findings (Williams and Coppelino, 2011), and further suggests that phosphorylation of the enzyme at Thr<sup>567</sup> is a key regulator of its endocytosis. Our studies focusing on Thr<sup>567</sup> build upon previously reported findings that expression of T567A-MT1-MMP-GFP mutants impairs cellular invasion and migration (Moss et al., 2009b; Williams and Coppelino, 2011). MT1-MMP phosphorylation on Tyr<sup>573</sup> has also been shown to play a role in tumor cell migration and MT1-MMP internalization (Uekita et al., 2001; Nyalendo et al., 2007; Moss et al., 2009a). A signaling pathway has been characterized involving LIMK1, which results in the phosphorylation of MT1-MMP on Tyr<sup>573</sup> (Lagoutte et al., 2016), and it is possible that this occurs in parallel to the pathway described here. Furthermore, it has previously been shown that expression of a Y573A mutant leads to reduced internalization of MT1-MMP owing to the fact that this residue resides in the binding site for the  $\mu$ 2 subunit of adaptor protein 2, a component of clathrin-mediated endocytosis (Uekita et al., 2001). These observations, combined with the results presented here, lead us to conclude that the upstream signaling mechanism resulting in Thr<sup>567</sup> phosphorylation is different from that of Tyr<sup>573</sup>, and future studies aim to elucidate whether this results in a clathrin-dependent or caveolar form of endocytosis.

It has been demonstrated previously that  $\beta$ 1 integrin associates with Src kinase and EGFR at the plasma membrane, and facilitates

their activation during tumor cell invasion (Moro et al., 2002; Williams and Coppelino, 2014). Adhesion of  $\beta 1$  integrin to the ECM signals the recruitment of Src kinase, and subsequently phosphorylation and activation of EGFR, independently of growth factors (Moro et al., 2002). In this study, we have determined that  $\beta 1$  integrin activation by the P4G11 antibody can stimulate activation of Src and EGFR as well as their association. Our observations of attenuated MT1-MMP phosphorylation when Src and EGFR are inhibited pharmacologically, as well as when Src is knocked down, despite activation of  $\beta 1$  integrin indicate that these two signaling molecules are necessary for  $\beta 1$  integrin-mediated activation of MT1-MMP. These results are consistent with previously published studies showing that inhibition of Src or EGFR (using the same inhibitors as used here) impairs invadopodia formation and consequent cell invasion (Yamaguchi et al., 2005; Chan et al., 2009; Liu et al., 2010; Hwang et al., 2011; Williams and Coppelino, 2014; Genna et al., 2018). We thus propose a possible mechanism for the regulation of MT1-MMP's internalization and recycling, wherein phosphorylation of the enzyme is regulated by signaling through  $\beta 1$  integrin, Src and EGFR. Because knockdown of Src did not result in a complete abrogation of EGFR tyrosine phosphorylation, we cannot conclude that Src is the only kinase responsible for activation of the receptor downstream of  $\beta 1$  integrin signaling. Indeed, other potential candidates involved in invadopodia biogenesis may be involved in this pathway, for example c-Met or p38 MAPK (Frey et al., 2006; Velpula et al., 2012; Saunders et al., 2015). Although our findings do not define recycling pathways that are specific for invadopodia, these structures do represent highly specialized subcellular membrane compartments (Hastie and Sherwood, 2016), and future characterization of potential unique recycling pathways associated with them will provide important advancement of our understanding of invadopodia biology.

In summary, we have demonstrated a mechanism by which activation of integrin receptors plays an essential role in the phosphorylation and subsequent internalization of MT1-MMP during cell invasion. Previous studies have identified association and functional cooperation between integrins and matrix metalloproteinases (Gálvez et al., 2002, 2003), and to these we now add the identification of a role for  $\beta 1$  integrin signaling in regulating MT1-MMP phosphorylation and activity. At this point, the kinase responsible for the phosphorylation of MT1-MMP in this model is not known, and future studies are aimed at determining this. Future work will also explore additional signaling molecules involved in the  $\beta 1$  integrin-MT1-MMP signaling pathway, as they may represent additional regulatory factors within the metastatic process that could be of interest as therapeutic targets.

## MATERIALS AND METHODS

### Reagents

Reagents and chemicals were purchased from Sigma-Aldrich or Fisher Scientific unless otherwise indicated. Antibodies to the following proteins were obtained from the indicated suppliers: GFP, MT1-MMP (ab290, ab51074; Abcam); phospho-serine/threonine, integrin  $\beta 1$  clone 9EG7 (612548; 553715; BD Biosciences); phospho-FAK-Tyr397 (3283; Cell Signaling Technology); AIB2, P4G11  $\beta 1$  integrin, P4C10, E7-s, hGAPDH-2G7 (Developmental Systems Hybridoma Bank); cortactin, Src-(active)-28; (PA1-9030; AHO0051; Fisher Scientific); TK55 (SH3 #4) (09-268; Millipore); EGFR, c-Src (B-12), c-Src (H-12) (sc-03; sc-8056; sc-5266; Santa Cruz Biotechnology); actin (A2228; Sigma-Aldrich); phospho-tyrosine clone 4G10, vinculin clone V284 (05-321; 05-386; Upstate Biotechnology). All fluorescently labeled secondary antibodies, Hoechst 33342, and Alexa Fluor 647-conjugated phalloidin were purchased from Life

Technologies. Src, FAK and control siRNA were purchased from Santa Cruz Biotechnology (sc-29228, sc-29310, and sc-37007, respectively).

### Cell culture and transfection

MDA-MB-231 and HT-1080 cells were obtained from the American Type Culture Collection (Manassas, VA, USA) and cultured in DMEM supplemented with 10% bovine calf serum (BCS). Growth conditions were kept at 37°C with humidity and a 5% CO<sub>2</sub> atmosphere. Cells were lifted using 5 mM EDTA/PBS (pH 7.4). Cells used in experiments were passaged between five and 20 times, and were passaged a maximum of 24 h prior to each experiment. Cells were plated in serum-free DMEM for 16 h prior to plating onto 0.2% gelatin-coated coverslips or culture plates in serum-free medium. Cells were treated with AIB2 (10  $\mu$ g ml<sup>-1</sup>), P4G11 (10  $\mu$ g ml<sup>-1</sup>), PP2 (10  $\mu$ M), AG1478 (11 nM) or EGF (60 ng ml<sup>-1</sup>) where indicated. Control conditions for all experiments were cells treated with the same concentration of a nonspecific IgG (E7-s). cDNAs for human wild-type Src, constitutively active Src (Y529F) and dominant-negative Src (K296R/Y528F) were obtained from Upstate Biotechnology.

cDNA for Y573A-MT1-MMP-GFP was obtained from GenScript, and the generation of MT1-MMP-GFP and T567A-MT1-MMP-GFP is described elsewhere (Williams and Coppelino, 2011). The pEGFP Rab5 and Rab7 were kind gifts from Dr John Brumell (Hospital for Sick Children, Toronto, Canada). Cells were transfected using jetPRIME Polyplus (VWR International) according to the protocol of the manufacturer. All transiently transfected constructs were expressed for 24 h. Cells were transfected with 50 nM siRNA and underwent knockdown for 48 h.

### Cell spreading assay

The cell spreading assay was performed as described previously (Iba et al., 2000). Briefly, glass coverslips were coated with 50  $\mu$ g ml<sup>-1</sup> poly-L-lysine/PBS, followed by 0.5% glutaraldehyde/PBS. Coverslips were then inverted onto a 70  $\mu$ l drop of 0.2% unlabeled gelatin/PBS. Cells were plated for 2 h at 50% confluency, then fixed and permeabilized. Coverslips were visualized by bright-field microscopy and images were captured. Image analysis was carried out using ImageJ software (National Institutes of Health).

### Boyden chamber migration and invasion assay

Cell culture inserts were prepared as described previously (Williams and Coppelino, 2014). Briefly, the bottoms of transwell inserts (8- $\mu$ m pore diameter, Corning) were coated with 20  $\mu$ g ml<sup>-1</sup> fibronectin/PBS. MDA-MB-231 cells were serum-starved for 24 h, lifted, seeded into chambers with simultaneous antibody treatment, and allowed to migrate for 20 h. The cells that invaded towards the lower chamber (10% BCS/0.1% BSA in DMEM) were fixed in 4% paraformaldehyde, stained with Hoechst 33342 for nuclear visualization, and counted. Cells that did not migrate through the membrane were removed with a cotton swab prior to fixation. Ten fields of cells per membrane were counted per treatment. Data are presented as percentage of control. For the invasion assay, the protocol was the same with the addition of coating the top of the chamber with 0.125 mg ml<sup>-1</sup> growth factor reduced Matrigel (BD Biosciences).

### Invadopodia formation assay

Invadopodium formation was performed as described previously (Williams et al., 2014). Glass coverslips were coated with 50  $\mu$ g ml<sup>-1</sup> poly-L-lysine/PBS, followed by 0.5% glutaraldehyde/PBS. The rationale for the use of a gelatin coating in this assay was that it is more amenable to imaging compared with substrates such as Matrigel, as described previously (Yu and Machesky, 2012). Coverslips were then inverted onto a 70  $\mu$ l drop of Alexa Fluor 594-labeled gelatin. The coverslips were then incubated with 5 mg ml<sup>-1</sup> sodium borohydride (Sigma-Aldrich) and then washed extensively in PBS. Tissue culture plates were coated similarly, with the exception being that 0.2% unlabeled gelatin/PBS was used. Cells were plated onto coverslips at 50% confluency and incubated for 4 h. Cells were fixed, permeabilized, and stained for an invadopodia marker (e.g. F-actin, TK55). Invadopodia were counted as spots of gelatin degradation overlaid by F-actin punctae as visualized by epifluorescence microscopy. Fifty cells per coverslip per treatment were scored for their ability to form invadopodia.

### Local gelatin degradation assay

Gelatin degradation assays were performed as described previously (Hoover et al., 2005). Briefly, coverslips were prepared as described under 'Invadopodia formation assay'. Cells were seeded at 30% confluency and incubated for 16 h or 24 h, as indicated. Cells were fixed, permeabilized, and stained for visualization. Gelatin degradation was quantified by measuring the area of degradation and scoring it as a percentage of total cell footprint. Alternatively, gelatin degradation was scored as described previously (Kean et al., 2009).

### Confocal immunofluorescence microscopy

Cells were serum-starved overnight and plated onto coverslips for 4 h or onto 0.2% gelatin-coated coverslips (as described under 'Invadopodia formation assay'). Cells were fixed in 4% paraformaldehyde/PBS and then washed in 150 mM glycine/PBS. Cells were permeabilized in 0.1% Triton X-100/PBS and blocked in 5% (w/v) BSA/PBS prior to antibody staining. Samples were imaged using a 63× (NA 1.4) lens on a Leica TCS SP2 system. Images were captured using Leica confocal software. Image processing and analysis was carried out using ImageJ software (National Institutes of Health). Alexa Fluor 594-labeled gelatin images were converted from red to white using ImageJ to improve the contrast of areas of degradation.

### Cell surface biotinylation

Cells that had been serum-starved overnight were plated onto 0.2% gelatin with simultaneous antibody treatment and incubated for the time period specified. Cells were then washed with ice-cold PBS (pH 7.4) once and incubated with 0.5 mg ml<sup>-1</sup> Sulfo-NHS-SS-Biotin (APEX-BIO) in 10 mM boric acid and 150 mM NaCl (pH 8.0) for 45 min at 4°C, turning once halfway through the incubation. The cells were then washed twice with 15 mM glycine/PBS to quench unreacted biotin and lysed using 1% Nonidet P-40, 10% glycerol, 0.5% sodium deoxycholate, 137 mM NaCl, 20 mM Tris-HCl (pH 8.0), 10 mM NaF, 10 mM Na<sub>2</sub>P<sub>4</sub>O<sub>7</sub>, 0.2 mM Na<sub>3</sub>VO<sub>4</sub> and protease inhibitor mixture. Lysate was incubated overnight with streptavidin-agarose beads (Novex, Thermo Fisher Scientific) at 4°C. Lysate was removed and beads were washed three times with cold lysis buffer. Proteins bound to the beads were eluted by boiling at 100°C in 2.5× Laemmli loading buffer.

### Biotin internalization assay

Cells were plated and surface labeled with biotin as described in 'Cell surface biotinylation'. Following incubation, cells were washed twice with 15 mM glycine/PBS and once with ice-cold PBS. Cells were then incubated in serum-free DMEM and simultaneous antibody treatment for 2 h at 37°C to allow for internalization of surface proteins. Cells were then washed with PBS and remaining surface biotin was cleaved by incubating cells for 25 min in an ice-cold solution containing 150 mM MeSNa/PBS (pH 8.2). Cells were washed three times with PBS and lysed as described above.

### MT1-MMP and β1 integrin trafficking

Protein trafficking assays were performed as described previously (Williams and Coppelino, 2011). Briefly, MDA-MB-231 cells expressing Rab5-GFP or Rab7-GFP were serum-starved overnight and plated onto gelatin-coated glass coverslips for 2 h to induce delivery of MT1-MMP β1 integrin to the cell surface. Cells were washed with ice-cold PBS and incubated with 1% BSA/PBS for 20 min at 4°C on ice to prevent internalization of surface proteins. Anti-MT1-MMP (8 μg ml<sup>-1</sup>) and anti-β1 integrin (5 μg ml<sup>-1</sup>) antibodies were added to the cells for 1 h. Cells were then rinsed with 0.2 M glycine/HCl (pH 5.0) followed by successive rinses with PBS to remove any unbound antibody. Cells were slowly warmed to 37°C in serum-free medium with or without antibody treatment for 40 min to induce internalization, then fixed and permeabilized. Samples were incubated with fluorescently labeled secondary antibodies in 1% BSA/PBS for 1 h and visualized by confocal microscopy. Colocalization analyses of MT1-MMP or β1 integrin with Rab5-GFP or Rab7-GFP were performed using the Coloc2 ImageJ plugin.

### Gelatin zymography

Overnight serum-starved cells were plated onto 0.2% gelatin in serum-free media with simultaneous antibody treatment for 16 h. Conditioned media

was collected and centrifuged to eliminate dead cells. Samples were prepared by adding 5× Laemmli buffer to 10 μg samples. Samples were run through a 7.5% acrylamide gel containing gelatin at 100 V to allow for band separation. The gel was then incubated in a wash buffer containing 2.5% Triton X-100, 50 mM Tris-HCl, 5 mM CaCl<sub>2</sub> and 1 μM ZnCl<sub>2</sub> (pH 7.5) at room temperature twice for 30 min at 75 rpm. The gel was then rinsed in an incubation buffer (similar to wash buffer listed above, with the exception that the final concentration of Triton X-100 was 1%) for 10 min at 75 rpm at room temperature. The gel was then incubated in fresh incubation buffer for 48 h at 37°C. The gel was stained with Coomassie Blue for 1 h at room temperature with agitation. The gel was then incubated with a de-staining solution of 40% methanol and 10% acetic acid until bands could be visualized. Densitometric analysis of band intensity was performed using ImageJ software and reported as a percentage of the control condition.

### Immunoprecipitation

Antibodies were coupled to protein G Dynabeads (Invitrogen) according to the manufacturer's instructions. Cells were lysed *in situ* with cold lysis buffer (described in 'Cell surface biotinylation'). Lysate was incubated with antibody-bound Dynabeads overnight at 4°C, then washed three times with ice-cold PBS. Proteins bound to the beads were eluted with 2.5× Laemmli loading buffer heated to 95°C. Immunoprecipitates were separated using SDS-PAGE and analyzed by western blot.

### Statistical analysis

The percentage of controls for three independent experimental replicates is shown with error bars representing the standard deviation. The mean is represented by the horizontal bar in all graphs. Analysis of western blot densitometry was performed using ImageJ software (National Institutes of Health). Images were scanned and the picture mode was changed to 'grayscale'. The region of interest was defined using the rectangle tool, and a rectangle was drawn to the minimum area that contained the entire band in the row. The measure tool was used to record pixel density in the region of interest, and this process was repeated using the same rectangle size for all conditions. For all experiments, each treatment group was compared with the control treatment by Student's *t*-test, with a statistical significance threshold of *P*=0.05. Treatments that differed significantly from the control (*P*<0.05) are indicated by an asterisk in the figures. Statistical analysis for all data was completed using Microsoft Excel. Graphs were prepared using GraphPad Prism 8.3.

### Competing interests

The authors declare no competing or financial interests.

### Author contributions

Conceptualization: O.R.G., M.G.C.; Methodology: O.R.G.; Validation: O.R.G.; Formal analysis: O.R.G., G.G., T.S., M.I.B.; Investigation: O.R.G., G.G., T.S.; Writing - original draft: O.R.G., M.G.C.; Writing - review & editing: O.R.G., M.G.C.; Visualization: M.G.C.; Supervision: M.G.C.; Project administration: M.G.C.; Funding acquisition: M.G.C.

### Funding

This work was supported by the Natural Sciences and Engineering Research Council of Canada (239122 to M.G.C.). O.R.G. holds a Queen Elizabeth II Graduate Scholarship in Science and Technology from the Ontario Ministry of Training Colleges and Universities.

### Supplementary information

Supplementary information available online at <http://jcs.biologists.org/lookup/doi/10.1242/jcs.239152.supplemental>

### Peer review history

The peer review history is available online at <https://jcs.biologists.org/lookup/doi/10.1242/jcs.239152.reviewer-comments.pdf>

### References

- Antelmi, E., Cardone, R. A., Greco, M. R., Rubino, R., Di Sole, F., Martino, N. A., Casavola, V., Carcangiu, M. L., Moro, L. and Reshkin, S. J. (2013). β1 integrin binding phosphorylates ezrin at T567 to activate a lipid raft signalsome driving invadopodia activity and invasion. *PLoS ONE* **8**, e75113. doi:10.1371/journal.pone.0075113



- Aoudjit, F. and Vuori, K. (2012). Integrin signaling in cancer cell survival and chemoresistance. *Chemother. Res. Pract.* **2012**, 1–16. doi:10.1155/2012/283181
- Artym, V. V., Yamada, K. M. and Mueller, S. C. (2009). ECM degradation assays for analyzing local cell invasion. (Even-Ram S., Artym, V.V., Eds). In *Methods in Molecular Biology*, 522 pp. 211–219. Humana Press.
- Beatty, B. T. and Condeelis, J. (2014). Digging a little deeper: the stages of invadopodium formation and maturation. *Eur. J. Cell Biol.* **93**, 438–444. doi:10.1016/j.ejcb.2014.07.003
- Beatty, B. T., Sharma, V. P., Bravo-Cordero, J. J., Simpson, M. A., Eddy, R. J., Koleske, A. J. and Condeelis, J. (2013).  $\beta 1$  integrin regulates Arg to promote invadopodial maturation and matrix degradation. *Mol. Biol. Cell* **24**, 1661–1675. doi:10.1091/mbc.e12-12-0908
- Bernardo, M. M. and Fridman, R. (2003). TIMP-2 (tissue inhibitor of metalloproteinase-2) regulates MMP-2 (matrix metalloproteinase-2) activity in the extracellular environment after pro-MMP-2 activation by MT1 (membrane type 1)-MMP. *Biochem. J.* **374**, 739–745. doi:10.1042/bj20030557
- Branch, K. M., Hoshino, D. and Weaver, A. M. (2012). Adhesion rings surround invadopodia and promote maturation. *Biol. Open* **1**, 711–722. doi:10.1242/bio.20121867
- Chan, K. T., Cortesio, C. L. and Huttenlocher, A. (2009). Fak alters invadopodia and focal adhesion composition and dynamics to regulate breast cancer invasion. *J. Cell Biol.* **185**, 357–370. doi:10.1083/jcb.200809110
- Deryugina, E. I., Ratnikov, B., Monosov, E., Postnova, T. I., DiScipio, R., Smith, J. W. and Strongin, A. Y. (2001). MT1-MMP initiates activation of pro-MMP-2 and integrin  $\alpha v \beta 3$  promotes maturation of MMP-2 in breast carcinoma cells. *Exp. Cell Res.* **263**, 209–223. doi:10.1006/excr.2000.5118
- Destaing, O., Planus, E., Bouvard, D., Oddou, C., Badowski, C., Bossy, V., Raducanu, A., Fourcade, B., Albiges-Rizo, C. and Block, M. R. (2010).  $\beta 1 A$  integrin is a master regulator of invadosome organization and function. *Mol. Biol. Cell* **21**, 4108–4119. doi:10.1091/mbc.e10-07-0580
- Destaing, O., Block, M. R., Planus, E. and Albiges-Rizo, C. (2011). Invadosome regulation by adhesion signaling. *Curr. Opin. Cell Biol.* **23**, 597–606. doi:10.1016/j.cob.2011.04.002
- Frey, M. R., Dise, R. S., Edelblum, K. L. and Polk, D. B. (2006). p38 kinase regulates epidermal growth factor receptor downregulation and cellular migration. *EMBO J.* **25**, 5683–5692. doi:10.1038/sj.emboj.7601457
- Frittoli, E., Palamidessi, A., Disanza, A. and Scita, G. (2011). Secretory and endo/exocytic trafficking in invadopodia formation: The MT1-MMP paradigm. *Eur. J. Cell Biol.* **90**, 108–114. doi:10.1016/j.ejcb.2010.04.007
- Gálvez, B. G., Matías-Román, S., Yáñez-Mó, M., Sánchez-Madrid, F. and Arroyo, A. G. (2002). ECM regulates MT1-MMP localization with  $\beta 1$  or  $\alpha v \beta 3$  integrins at distinct cell compartments modulating its internalization and activity on human endothelial cells. *J. Cell Biol.* **159**, 509–521. doi:10.1083/jcb.200205026
- Gálvez, B., Matías-Román, S., Yáñez-Mó, M., Vicente-Manzanares, M., Sánchez-Madrid, F. and Arroyo, A. (2003). Caveolae are a novel pathway for membrane-type 1 matrix metalloproteinase traffic in human endothelial cells. *Mol. Biol. Cell* **15**, 678–687. doi:10.1091/mbc.e03-07-0516
- Ganguly, K. K., Pal, S., Moulik, S. and Chatterjee, A. (2013). Integrins and metastasis. *Cell Adhes. Migr.* **7**, 251–261. doi:10.4161/cam.23840
- Genna, A., Lapetina, S., Lukic, N., Twafra, S., Meirson, T., Sharma, V. P., Condeelis, J. S. and Gil-Henn, H. (2018). Pyk2 and FAK differentially regulate invadopodia formation and function in breast cancer cells. *J. Cell Biol.* **217**, 375–395. doi:10.1083/jcb.201702184
- Guo, W. and Giancotti, F. G. (2004). Integrin signalling during tumour progression. *Nat. Rev. Mol. Cell Biol.* **5**, 816–826. doi:10.1038/nrm1490
- Hastie, E. L. and Sherwood, D. R. (2016). A new front in cell invasion: the invadopodial membrane. *Eur. J. Cell Biol.* **95**, 441–448. doi:10.1016/j.ejcb.2016.06.006
- Hoover, H., Muralidharan-Chari, V., Tague, S. and D'Souza-Schorey, C. (2005). Investigating the role of ADP-ribosylation factor 6 in tumor cell invasion and extracellular signal-regulated kinase activation. *Methods Enzymol.* **404**, 134–147. doi:10.1016/S0076-6879(05)04014-0
- Hwang, Y. S., Park, K.-K. and Chung, W.-Y. (2011). Invadopodia formation in oral squamous cell carcinoma: the role of epidermal growth factor receptor signalling. *Arch. Oral Biol.* **57**, 335–343. doi:10.1016/j.archoralbio.2011.08.019
- Hynes, R. O. (2002). Integrins: bidirectional, allosteric signalling machines in their roles as major adhesion receptors. *Cell* **110**, 673–687. doi:10.1016/S0092-8674(02)00971-6
- Iba, K., Albrechtsen, R., Gilpin, B., Fröhlich, C., Loechel, F., Zolkiewska, A., Ishiguro, K., Kojima, T., Liu, W., Langford, J. K. et al. (2000). The cysteine-rich domain of human ADAM 12 supports cell adhesion through syndecans and triggers signaling events that lead to  $\beta 1$  integrin-dependent cell spreading. *J. Cell Biol.* **149**, 1143–1155. doi:10.1083/jcb.149.5.1143
- Kean, M. J., Williams, K. C., Skalski, M., Myers, D., Burtinik, A., Foster, D. and Coppolino, M. G. (2009). VAMP3, syntaxin-13 and SNAP23 are involved in secretion of matrix metalloproteinases, degradation of the extracellular matrix and cell invasion. *J. Cell Sci.* **122**, 4089–4098. doi:10.1242/jcs.052761
- Kuwada, S. K. and Li, X. (2000). Integrin  $\alpha 5 / \beta 1$  mediates fibronectin-dependent epithelial cell proliferation through epidermal growth factor receptor activation. *Mol. Biol. Cell* **11**, 2485–2496. doi:10.1091/mbc.11.7.2485
- Lagoutte, E., Villeneuve, C., Lafanechère, L., Wells, C. M., Jones, G. E., Chavrier, P. and Rossé, C. (2016). LIMK regulates tumor-cell invasion and matrix degradation through tyrosine phosphorylation of MT1-MMP. *Sci. Rep.* **6**, 24925. doi:10.1038/srep24925
- Lehti, K., Valtanen, H., Wickström, S., Lohi, J. and Keski-Oja, J. (2000). Regulation of membrane-type-1 matrix metalloproteinase activity by its cytoplasmic domain. *J. Biol. Chem.* **275**, 15006–15013. doi:10.1074/jbc.M910220199
- Liu, S., Yamashita, H., Weidow, B., Weaver, A. M. and Quaranta, V. (2010). Laminin-332 -  $\beta 1$  Integrin interactions negatively regulate invadopodia. *J. Cell. Physiol.* **223**, 134–142. doi:10.1002/jcp.22018
- Lu, P., Weaver, V. M. and Werb, Z. (2012). The extracellular matrix: a dynamic niche in cancer progression. *J. Cell Biol.* **196**, 395–406. doi:10.1083/jcb.201102147
- Mitra, S. K. and Schlaepfer, D. D. (2006). Integrin-regulated FAK-Src signaling in normal and cancer cells. *Curr. Opin. Cell Biol.* **18**, 516–523. doi:10.1016/j.cob.2006.08.011
- Moro, L., Venturino, M., Bozzo, C., Silengo, L., Altruda, F., Beguinot, L., Tarone, G. and Defilippi, P. (1998). Integrins induce activation of EGF receptor: role in MAP kinase induction and adhesion-dependent cell survival. *EMBO J.* **17**, 6622–6632. doi:10.1093/emboj/17.22.6622
- Moro, L., Dolce, L., Cabodi, S., Bergatto, E., Boeri Erba, E., Smeriglio, M., Turco, E., Retta, S. F., Giuffrida, M. G., Venturino, M. et al. (2002). Integrin-induced epidermal growth factor (EGF) receptor activation requires c-Src and p130Cas and leads to phosphorylation of specific EGF receptor tyrosines. *J. Biol. Chem.* **277**, 9405–9414. doi:10.1074/jbc.M109101200
- Moss, N. M., Liu, Y., Johnson, J. J., Debiase, P., Jones, J., Hudson, L. G., Munshi, H. G. and Stack, M. S. (2009a). Epidermal growth factor receptor-mediated membrane type 1 matrix metalloproteinase endocytosis regulates the transition between invasive versus expansive growth of ovarian carcinoma cells in three-dimensional collagen. *Mol. Cancer Res.* **7**, 809–820. doi:10.1158/1541-7786.MCR-08-0571
- Moss, N. M., Wu, Y. I., Liu, Y., Munshi, H. G. and Stack, M. S. (2009b). Modulation of the membrane type 1 matrix metalloproteinase cytoplasmic tail enhances tumor cell invasion and proliferation in three-dimensional collagen matrices. *J. Biol. Chem.* **284**, 19791–19799. doi:10.1074/jbc.M109.020362
- Murphy, D. A. and Courtneidge, S. A. (2011). The 'ins' and 'outs' of podosomes and invadopodia: characteristics, formation and function. *Nat. Rev. Mol. Cell Biol.* **12**, 413–426. doi:10.1038/nrm3141
- Nagase, H., Visse, R. and Murphy, G. (2006). Structure and function of matrix metalloproteinases and TIMPs. *Cardiovasc. Res.* **69**, 562–573. doi:10.1016/j.cardiores.2005.12.002
- Nakahara, H., Mueller, S. C., Nomizu, M., Yamada, Y., Yeh, Y. and Chen, W. T. (1998). Activation of beta1 integrin signaling stimulates tyrosine phosphorylation of p190RhoGAP and membrane-protrusive activities at invadopodia. *J. Biol. Chem.* **273**, 9–12. doi:10.1074/jbc.273.1.9
- Nyalendo, C., Michaud, M., Beaulieu, E., Roghi, C., Murphy, G., Gingras, D. and Béliveau, R. (2007). Src-dependent phosphorylation of membrane type I matrix metalloproteinase on cytoplasmic tyrosine 573: Role in endothelial and tumor cell migration. *J. Biol. Chem.* **282**, 15690–15699. doi:10.1074/jbc.M608045200
- Poincloux, R., Lizarraga, F. and Chavrier, P. (2009). Matrix invasion by tumour cells: a focus on MT1-MMP trafficking to invadopodia. *J. Cell Sci.* **122**, 3015–3024. doi:10.1242/jcs.034561
- Remacle, A., Murphy, G. and Roghi, C. (2003). Membrane type I-matrix metalloproteinase (MT1-MMP) is internalised by two different pathways and is recycled to the cell surface. *J. Cell Sci.* **116**, 3905–3916. doi:10.1242/jcs.00710
- Saunders, V. C., Lafitte, M., Adrados, I., Quereda, V., Feurstein, D., Ling, Y. Y., Fallahi, M., Rosenberg, L. H. and Duckett, D. R. (2015). Identification of an EGFRvIII-JNK2-HGF/c-Met-signaling axis required for intercellular crosstalk and glioblastoma multiforme cell invasion. *Mol. Pharmacol.* **88**, 962–969. doi:10.1124/mol.115.097774
- Tang, Y., Rowe, R. G., Botvinick, E. L., Kurup, A., Putnam, A. J., Seiki, M., Weaver, V. M., Keller, E. T., Goldstein, S., Dai, J. et al. (2013). MT1-MMP-dependent control of skeletal stem cell commitment via a  $\beta 1$ -integrin/YAP/TAZ signaling axis. *Dev. Cell* **25**, 402–416. doi:10.1016/j.devcel.2013.04.011
- Toth, M., Chvyrkova, I., Bernardo, M. M., Hernandez-Barrantes, S. and Fridman, R. (2003). Pro-MMP-9 activation by the MT1-MMP/MMP-2 axis and MMP-3: role of TIMP-2 and plasma membranes. *Biochem. Biophys. Res. Commun.* **308**, 386–395. doi:10.1016/S0006-291X(03)01405-0
- Uekita, T., Itoh, Y., Yana, I., Ohno, H. and Seiki, M. (2001). Cytoplasmic tail-dependent internalization of membrane-type 1 matrix metalloproteinase is important for its invasion-promoting activity. *J. Cell Biol.* **155**, 1345–1356. doi:10.1083/jcb.200108112
- Velpula, K. K., Dasari, V. R., Asuthkar, S., Gorantla, B. and Tsung, A. J. (2012). EGFR and c-Met cross talk in glioblastoma and its regulation by human cord blood stem cells. *Transl. Oncol.* **5**, 379–392. doi:10.1593/tlo.12235
- Wang, F., Weaver, V. M., Petersen, O. W., Larabell, C. A., Dedhar, S., Briand, P., Lupu, R. and Bissell, M. J. (1998). Reciprocal interactions between  $\beta 1$  integrin and epidermal growth factor receptor in three-dimensional basement breast cultures: a different perspective in epithelial biology. *Cell Biol.* **95**, 1–6. doi:10.1073/pnas.95.25.14821

- Wang, X., Ma, D., Keski-Oja, J. and Pei, D.** (2004). Co-recycling of MT1-MMP and MT3-MMP through the trans-Golgi network. Identification of DKV582 as a recycling signal. *J. Biol. Chem.* **279**, 9331-9336. doi:10.1074/jbc.M312369200
- Weaver, A. M.** (2006). Invadopodia: specialized cell structures for cancer invasion. *Clin. Exp. Metastasis* **23**, 97-105. doi:10.1007/s10585-006-9014-1
- Williams, K. C. and Coppelino, M. G.** (2011). Phosphorylation of membrane type 1-matrix metalloproteinase (MT1-MMP) and its vesicle-associated membrane protein 7 (VAMP7)-dependent trafficking facilitate cell invasion and migration. *J. Biol. Chem.* **286**, 43405-43416. doi:10.1074/jbc.M111.297069
- Williams, K. C. and Coppelino, M. G.** (2014). SNARE-dependent interaction of Src, EGFR and 1 integrin regulates invadopodia formation and tumor cell invasion. *J. Cell Sci.* **127**, 1712-1725. doi:10.1242/jcs.134734
- Williams, K. C., McNeilly, R. E. and Coppelino, M. G.** (2014). SNAP23, Syntaxin4, and vesicle-associated membrane protein 7 (VAMP7) mediate trafficking of membrane type 1-matrix metalloproteinase (MT1-MMP) during invadopodium formation and tumor cell invasion. *Mol. Biol. Cell* **25**, 2061-2070. doi:10.1091/mbc.e13-10-0582
- Wisdom, K. M., Adebawale, K., Chang, J., Lee, J. Y., Nam, S., Desai, R., Rossen, N. S., Rafat, M., West, R. B., Hodgson, L. et al.** (2018). Matrix mechanical plasticity regulates cancer cell migration through confining microenvironments. *Nat. Commun.* **9**, 4144. doi:10.1038/s41467-018-06641-z
- Yamaguchi, H., Lorenz, M., Kempia, S., Sarmiento, C., Coniglio, S., Symons, M., Segall, J., Eddy, R., Miki, H., Takenawa, T. et al.** (2005). Molecular mechanisms of invadopodium formation: The role of the N-WASP-Arp2/3 complex pathway and cofilin. *J. Cell Biol.* **168**, 441-452. doi:10.1083/jcb.200407076
- Yu, X. and Machesky, L. M.** (2012). Cells assemble invadopodia-like structures and invade into matrigel in a matrix metalloprotease dependent manner in the circular invasion assay. *PLoS ONE* **7**, e30605. doi:10.1371/journal.pone.0030605
- Yu, X., Miyamoto, S. and Mekada, E.** (2000). Integrin  $\alpha 2\beta 1$ -dependent EGF receptor activation at cell-cell contact sites. *J. Cell Sci.* **113**, 2139-2147.

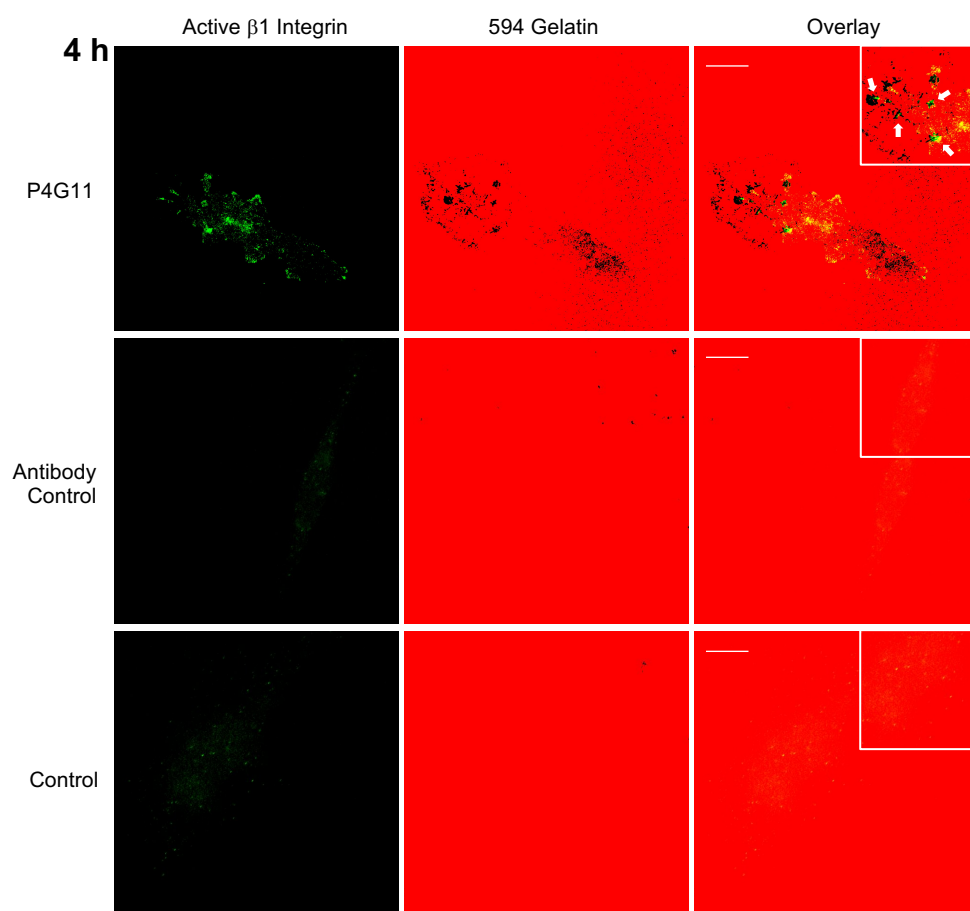


**Figure S1.** Cells Treated with P4G11 Display Colocalization of Active  $\beta 1$  Integrin and Areas of Gelatin Degradation. MDA-MB-231 cells were serum-starved for 24 hours, then plated onto fluorescent gelatin-coated coverslips for 4 hours with simultaneous antibody treatment. Cells were then fixed, permeabilized, and stained for active  $\beta 1$  integrin. Cells were analyzed by confocal microscopy. A representative section from the ventral region of a cell is shown. White arrows indicate areas of colocalization. All data represent three or more biological replicates with at least three technical replicates. Scale bar, 10  $\mu$ m.



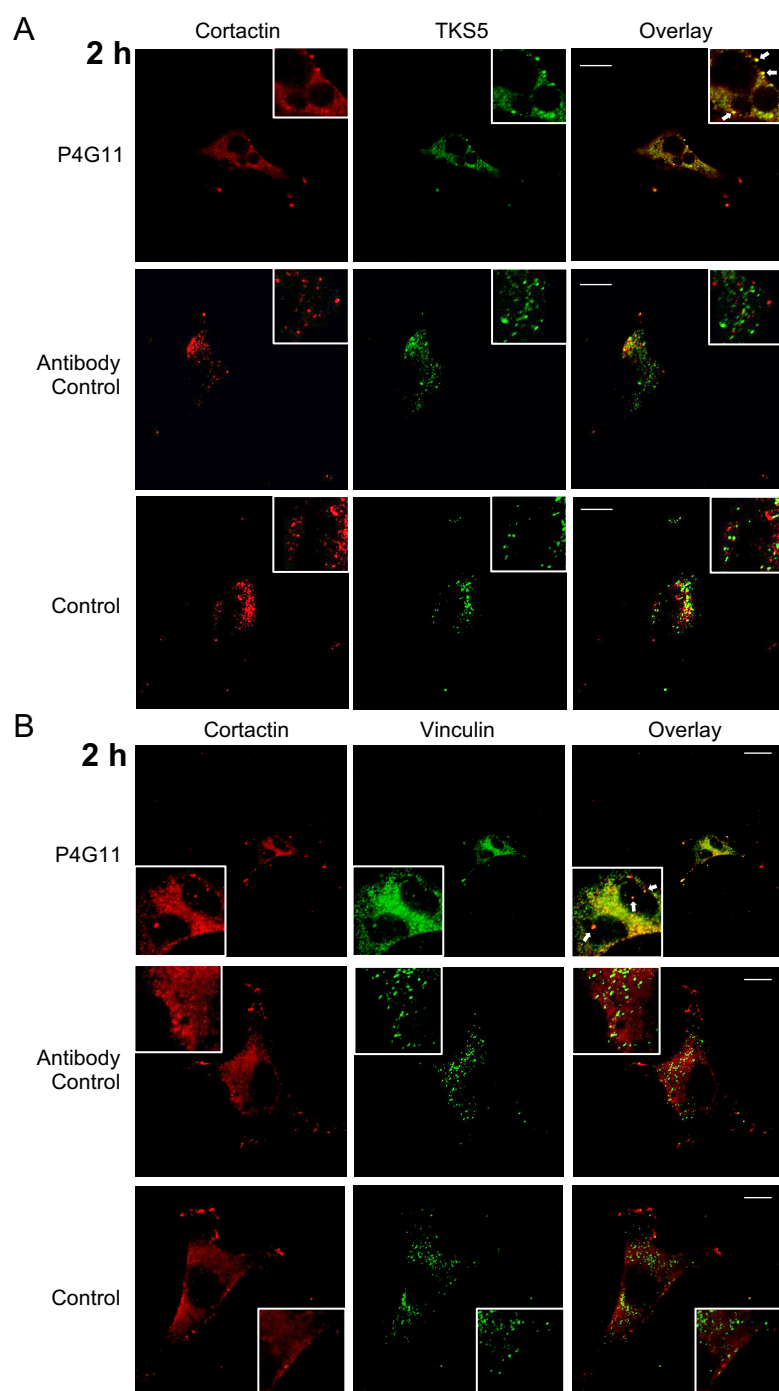


**Figure S2.** Cells Treated with P4G11 Display Colocalization of Invadopodia Precursor Markers. Cells were serum-starved for 24 hours, then seeded onto coverslips for 2 hours with antibody treatment, then fixed, permeabilized, and stained for (A) cortactin and TKS5, or (B) cortactin and vinculin. Cells were analyzed by confocal microscopy. A representative section from the ventral region of a cell is shown. White arrows indicate invadopodia precursors as defined by overlay of stained proteins. All data represent three or more biological replicates with at least three technical replicates. Scale bar, 10  $\mu$ m.

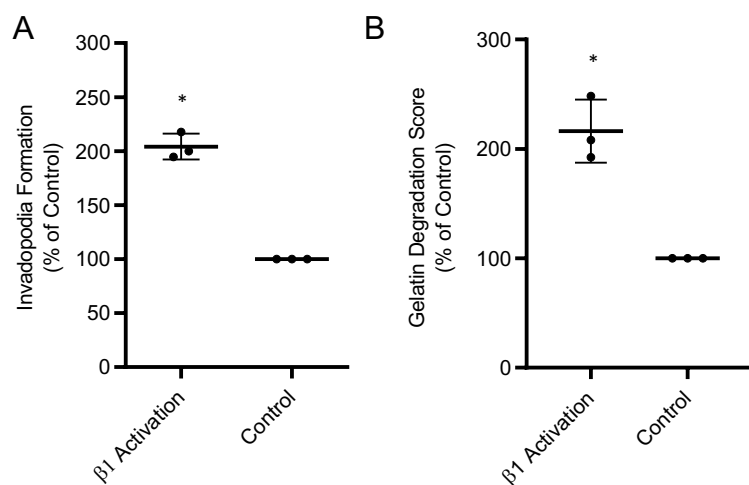


**Figure S3.**  $\beta 1$  Integrin Activation Increases Invadopodium Formation and Local Gelatin Degradation in HT-1080 Cells. Cells were serum-starved, treated with P4G11, and plated on fluorescently labelled gelatin-coated coverslips for 4 h (A) or 16 h (B). A, Quantification of invadopodium formation. Cells with F-actin puncta overlaying dark spots of gelatin degradation were counted as cells forming invadopodia. B, Quantification of gelatin degradation. Cells were analyzed for dark areas of degradation and scored as described under "Experimental Procedures." The percentages of cells are shown from experiments in which 50 cells/sample were analyzed and normalized to the control condition. All data are presented as percent of control  $\pm$  S.D. All data represent three or more biological replicates with at least three technical replicates. Asterisks denote values significantly different from control (\*,  $p < 0.05$ ).

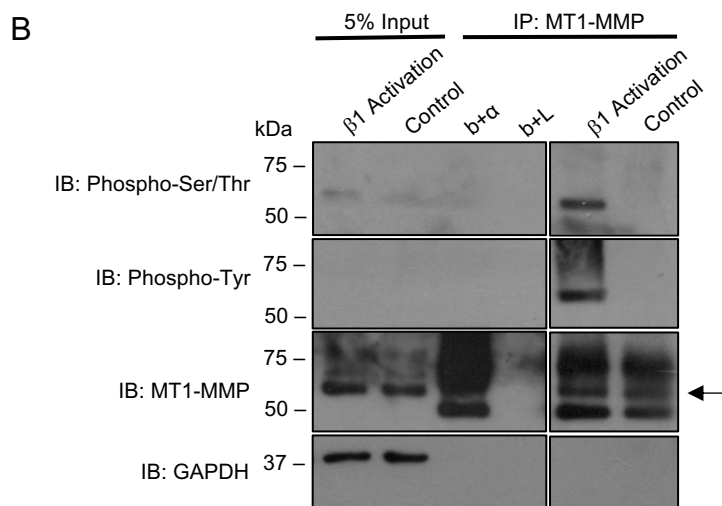
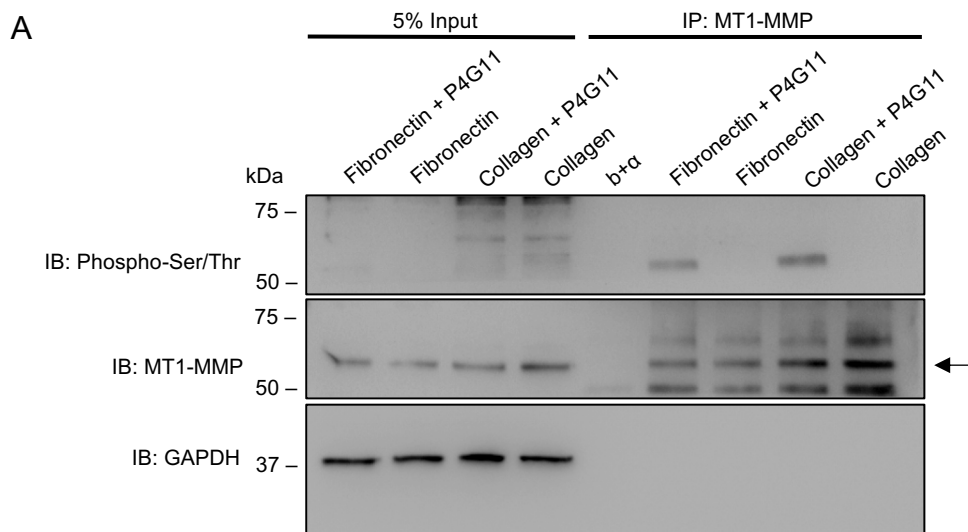


**Figure S4.** Activation of  $\beta$ 1 Integrin Induces Phosphorylation of MT1-MMP on Both Fibronectin and Collagen Substrates, and in HT-1080 Cells Plated on Gelatin. **A**, Cell culture plates were coated with either fibronectin ( $5 \mu\text{g cm}^{-2}$ ) or collagen type I ( $10 \mu\text{g cm}^{-2}$ ), and serum-starved cells were plated for 2 h with or without treatment of P4G11. **B**, HT-1080 cells were plated onto gelatin-coated cell culture plates for 2 h with or without treatment of P4G11. Immunoprecipitates of MT1-MMP were analyzed by Western blot for phospho-Ser/Thr (**A**, **B**) and phospho-Tyr (**B**), and the phospho-Ser/Thr blot was then stripped and re-probed for MT1-MMP. Arrow indicates the active form of MT1-MMP immunoprecipitated from the lysate. *Control* cells were treated with a non-specific supernatant antibody. b+L, beads plus lysate; b+ $\alpha$ , beads plus antibody.



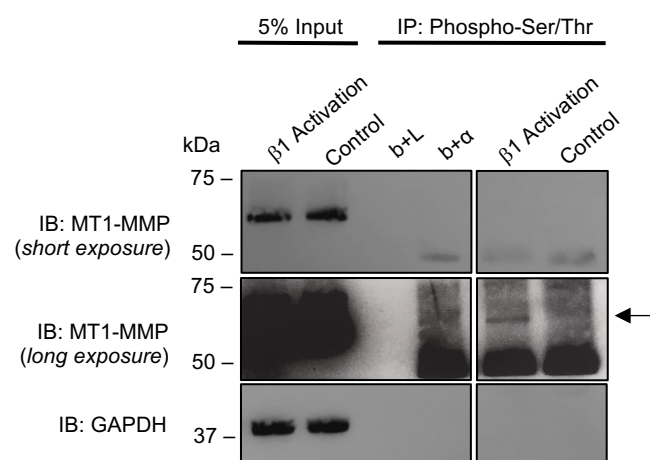


**Figure S5.** Activation of  $\beta 1$  Integrin Induces Phosphorylation of MT1-MMP. A, Immunoprecipitation of Phospho-Ser/Thr from MDA-MB-231 cells. Cells were plated onto gelatin-coated cell culture plates for 2 h, with or without treatment of P4G11, and immunoprecipitates of phospho-Ser/Thr were analyzed by Western blot for MT1-MMP. Arrow indicates immunoprecipitated MT1-MMP. *Control* cells were treated with a non-specific supernatant antibody. *b+L*, beads plus lysate; *b+α*, beads plus antibody. All data represent three or more biological replicates with at least three technical replicates.

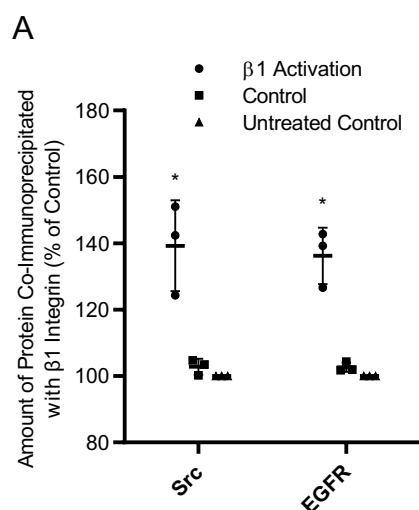


**Figure S6.** Treatment with P4G11 Increases the Colocalization and Association of Invadopodial Proteins. Serum-starved MDA-MB-231 cells were plated onto gelatin for 2 hours with or without treatment with P4G11. Immunoprecipitates of  $\beta 1$  integrin were analyzed for association with Src kinase and EGFR by Western blot and quantified. All data are presented as percent of control  $\pm$  S.D. Asterisks denote values significantly different from the control condition (\*,  $p < 0.05$ ). All data represent three or more biological replicates with at least three technical replicates.

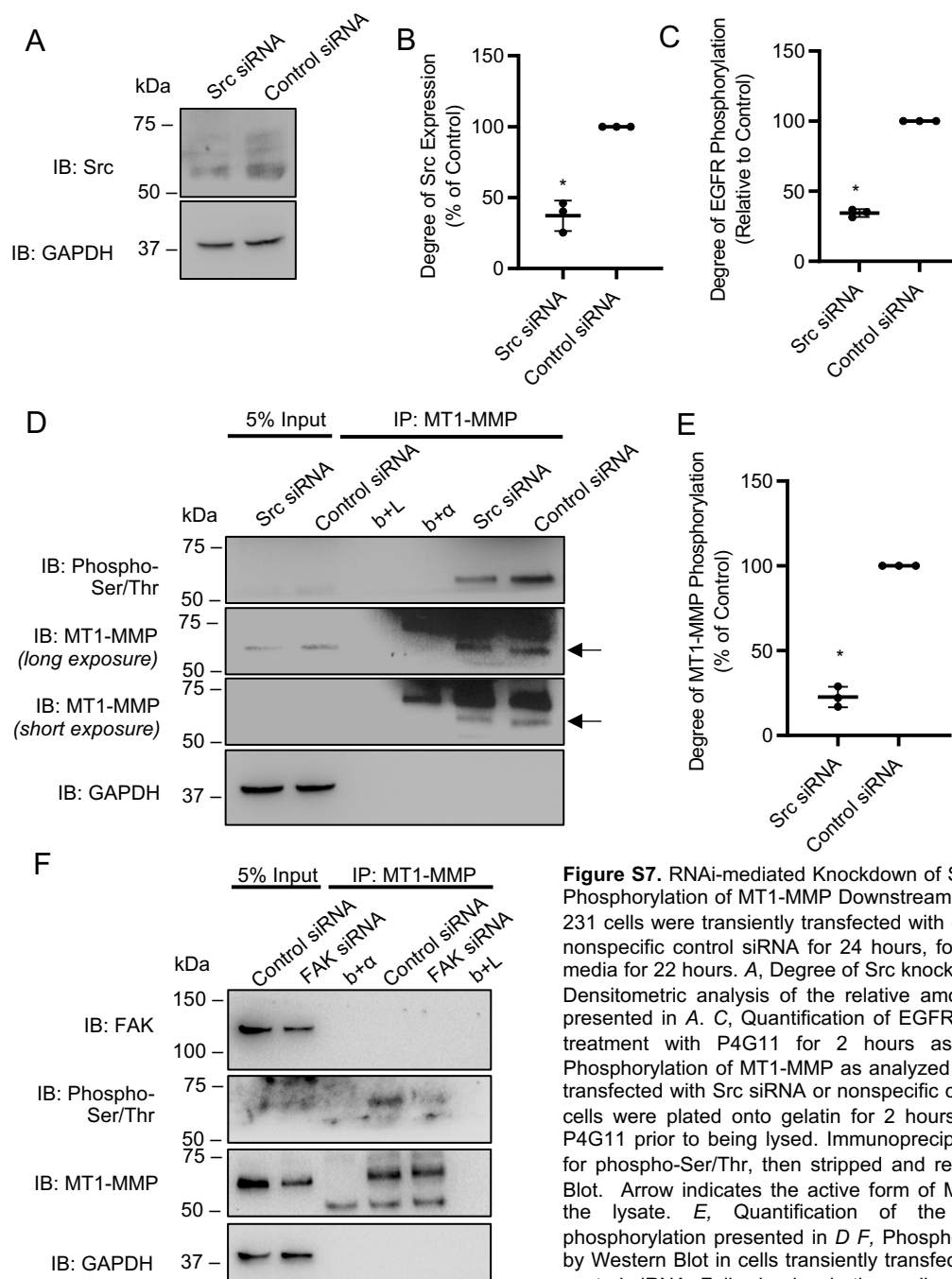


**Figure S7.** RNAi-mediated Knockdown of Src Kinase and FAK Decreases the Phosphorylation of MT1-MMP Downstream of  $\beta 1$  Integrin Activation. MDA-MB-231 cells were transiently transfected with either siRNA targeting Src, FAK, or nonspecific control siRNA for 24 hours, followed by incubation in serum-free media for 22 hours. **A**, Degree of Src knockdown assessed by Western blot. **B**, Densitometric analysis of the relative amount of Src expressed by cells as presented in **A**. **C**, Quantification of EGFR tyrosine phosphorylation following treatment with P4G11 for 2 hours as analyzed by Western Blot. **D**, Phosphorylation of MT1-MMP as analyzed by Western Blot in cells transiently transfected with Src siRNA or nonspecific control siRNA. Following incubation, cells were plated onto gelatin for 2 hours with simultaneous treatment with P4G11 prior to being lysed. Immunoprecipitates of MT1-MMP were analyzed for phospho-Ser/Thr, then stripped and re-probed for MT1-MMP by Western Blot. Arrow indicates the active form of MT1-MMP immunoprecipitated from the lysate. **E**, Quantification of the relative degree of MT1-MMP phosphorylation presented in **D**. **F**, Phosphorylation of MT1-MMP as analyzed by Western Blot in cells transiently transfected with FAK siRNA or nonspecific control siRNA. Following incubation, cells were plated onto gelatin for 2 hours with simultaneous treatment with P4G11 prior to being lysed. Immunoprecipitates of MT1-MMP were analyzed for phospho-Ser/Thr, then stripped and re-probed for MT1-MMP by Western Blot. *b+L*, beads plus lysate; *b+α*, beads plus antibody. All data represent three or more biological replicates with at least three technical replicates.



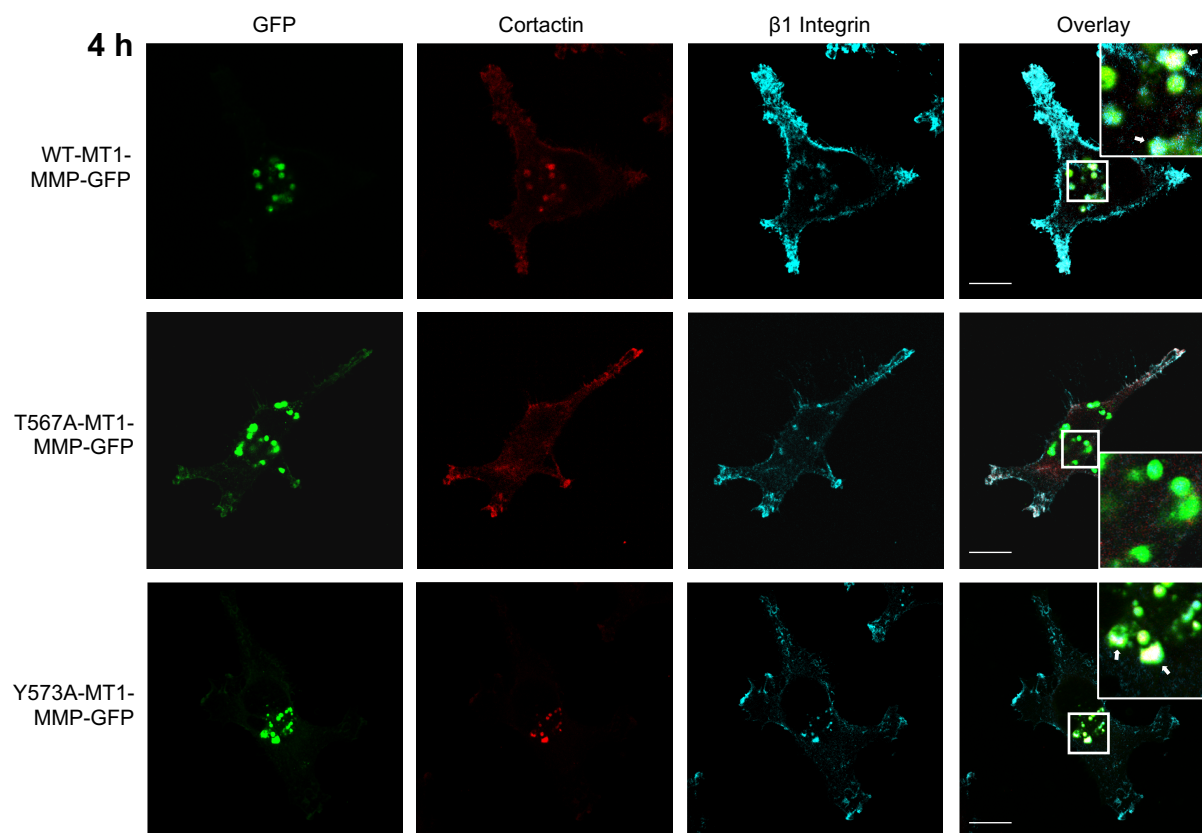


**Figure S8.** Cells Expressing an MT1-MMP Threonine-567 Mutant Demonstrate Decreased Association Between the GFP-tagged Construct, Cortactin, and  $\beta 1$  Integrin, and Decreased Invadopodium Formation. Cells transfected with WT-MT1-MMP-GFP, T567A-MT1-MMP-GFP, or Y573A-MT1-MMP-GFP were serum-starved and treated with P4G11 and plated onto gelatin-coated coverslips for 4 h. Cells were then fixed, permeabilized, and stained for cortactin and  $\beta 1$  integrin, and analyzed by confocal microscopy. White arrows in the zoomed region indicate overlap of all three proteins. All data represent three or more biological replicates with at least three technical replicates. Scale bar, 10  $\mu$ m.